European Journal of Soil Science

SPECIAL ISSUE EJP SOIL Special Issue – Climate-Smart Sustainable Agricultural Soil Management for the Future - III

WILEY

RESEARCH ARTICLE OPEN ACCESS

Site-Specific Climate Impacts Outweigh No-Till Benefits for Modelled Winter Wheat Yields Across a European Gradient

Katharina Hildegard Elisabeth Meurer[1] | Maria Eliza Turek[2,3] | Johannes Wilhelmus Maria Pullens[4] | Edberto Moura-Lima[5,6] | Jeroen D. M. Schreel[7] | Annelie Holzkämper[2,3] | Bano Mehdi-Schulz[5]

[1]Department of Soil and Environment, Swedish University of Agricultural Sciences – SLU, Uppsala, Sweden | [2]Agroscope, Zürich, Switzerland | [3]Oeschger Centre for Climate Change Research, University of Bern, Bern, Switzerland | [4]Department of Agroecology, Aarhus University, Tjele, Denmark | [5]University of Natural Resources and Life Sciences, Vienna (BOKU), Institute of Hydrology and Water Management, Vienna, Austria | [6]BAW Research, Petzenkirchen, Austria | [7]Flanders Research Institute for Agriculture, Fisheries and Food (ILVO), Melle, Belgium

Correspondence: Katharina Hildegard Elisabeth Meurer (katharina.meurer@slu.se)

Received: 29 August 2025 | **Revised:** 20 May 2026 | **Accepted:** 23 May 2026

Keywords: climate change adaptation | long-term field experiments | model ensemble | projected climate | soil management practices

ABSTRACT

Sustainable soil management practices, including conservation tillage practices, such as reduced tillage and no-till, are considered beneficial for different soil functions. So far, additional benefits of applying conservation tillage to improve crop yields under climate change are not fully clear and have rarely been investigated, particularly how potential benefits vary over time and under different pedo-climatic conditions. Using a cross-site and multi-model setup with four agro-hydrological models, this study sheds light on the questions whether, when, and where adaptation benefits of conservation tillage can be expected under future climate scenarios (time period 2020–2090, shared socio-economic pathways ssp2-4.5 and ssp5-8.5). To evaluate these questions, we used observations from three long-term experimental field trials in Denmark, Switzerland, and Austria to assess the benefits of no-till compared to conventional tillage regarding winter wheat (*Triticum aestivum* L.) productivity and soil hydrology, including key water balance components, such as actual evapotranspiration, percolation, and surface runoff. Our results suggest that the influence of climate scenarios of the respective sites overcome the potential benefits of the tillage management. While the simulated yields and water balance components showed different trends at the three sites, the intensity of the change was mainly driven by the climate models, where the climate model projecting the most intense changes in terms of temperature and precipitation most often also resulted in shorter growing periods and, related to that, higher yield losses. Therefore, no robust estimates of the adaptation benefits of no-till practices on winter wheat productivity could be quantified based on model ensemble projections, indicating stability in grain yields regardless of the tillage management. In general, the study results suggest that tillage as only adaptation measure is not sufficient to minimize future climate change-derived yield gaps and, consequently, ensure food security. Further work should explore the use of site-specific agricultural technologies, such as precision farming and variable rate application, as well as adaptation of (different) crops through targeted breeding for local conditions.

1 | Introduction

Continuous increase in crop yields is required to feed the growing world population. In Europe, wheat production has a high priority, as 34% of the global wheat production and 28% of the global wheat production area were located in Europe in 2023 (FAOSTAT 2023). This production will be affected by a future climate (Trnka et al. 2014; Ewert et al. 2005; Asseng et al. 2015; Bracho-Mujica et al. 2024), which is often projected to bring higher temperatures over longer periods, as well as changes in precipitation patterns, resulting in both longer droughts and extreme rainfall events. In addition,

> **Highlights**
>
> - Four agro-hydrological models were used to simulate winter wheat yields at three European sites.
> - Yield trends differed by site but were mainly driven by the projected climate.
> - Adaptation benefits of no-till are small across sites.
> - Site-specific adaptation strategies, including crop breeding and precision technologies, are needed.

intensive field management practices, including soil cultivation, fertilizer, and herbicide application, put great pressure on agricultural soils and have a major impact on the surrounding environment (Holland 2004; Soane et al. 2012; Kopittke et al. 2019). Unsustainable management practices, for example (deep) tillage, usage of heavy machinery, and overgrazing, lead to gradual soil degradation, primarily evidenced by a reduction in soil functioning and various ecosystem services, one of them being crop productivity (Diacono and Montemurro 2010). Directly visible consequences are, for example, the destruction of soil structure and the associated deterioration of the soil's water storage capacity, in turn increasing soil erosion. The resulting reductions in crop growth and yield provide less organic matter to the soil, which in turn influences the structure and hydraulic functions of the soil negatively, driving the vicious circle of soil degradation (Meurer, Barron, et al. 2020). Thus, maintaining high crop yields without further harming the soil will benefit soil carbon storage, soil structure, and soil water retention in the long term (Six et al. 2000).

More conservative soil management practices, including reduced tillage and no-till, have been shown to benefit soil structure, water retention (Pagliai et al. 2004), and reduced nitrate leaching (Hansen et al. 2015), and are generally assumed to improve the climatic resilience of cropping systems to drought (Ogle et al. 2019). The impacts of specific management practices on selected soil or plant parameters have been summarized and evaluated in numerous meta-analyses (Meurer et al. 2018; Peixoto et al. 2020), with different practices generally being considered beneficial, disadvantageous, or without any effect on the target variable(s). Recently, a synthesis of these meta-analyses indicated conflicting results: Blanchy et al. (2023) synthesized 127 European meta-analyses that investigated synergies and trade-offs to help explain the effects of soil and crop management in terms of the underlying processes and mechanisms. Overall, soil conservation practices, such as the addition of organic soil amendments, as well as practices that maintain continuous living cover, provided significant benefits for soil water regulation due to improved soil aggregation and enhanced bio-porosity created by soil fauna. In a global meta-analysis, Pittelkow et al. (2015) showed that crop yields were generally 4%–12% lower under no-till compared to conventional management. However, these observations depended strongly on crop type and environmental conditions. For example, no-tillage performed best under rainfed conditions in dry climates, matching conventional tillage yields on average. Despite these advantages at the local scale, the benefits of reduced tillage as a climate change adaptation strategy are not completely clear, and trade-offs, such as nitrogen losses through leaching or greenhouse gas emissions, may occur (Blanchy et al. 2023).

The impacts of conservational management practices, such as minimal soil disturbance, permanent plant cover, and crop rotations, on soil hydrological and biological functioning, as well as crop performance have been studied in numerous long-term field experiments (LTEs) around the world. These experiments are commonly used to test hypotheses related to agronomical research questions and to adapt and evaluate management strategies. With that, they can provide valuable information and provide insights into the combined effects of (i) weather and climatic change and (ii) management practices on target parameters, such as soil organic carbon, hydrology, and crop yield. The number and distribution of existing LTEs across Europe (Blanchy et al. 2024) gives the possibility to evaluate the same or similar management practices under different pedo-climatic conditions, thus enabling the development of site-specific adaptation measures. With climate change becoming more and more perceptible, it is of utmost importance to accurately understand and predict potential feedback mechanisms in the soil–plant-atmosphere continuum in order to develop effective adaptation strategies. Here, mechanistic models can provide insights into soil and crop processes in future climates predicted and over a long period of time.

Multi-model comparisons and model ensembles have been recognized as effective methods in climate change research (Duan et al. 2019), also related to agriculture and potential impacts of future climate. For example, in a global analysis of climate change impacts on crop yields, Jägermeyr et al. (2021) applied a suite of agro-ecosystem models at 0.5° grid resolution to simulate four major crops (maize (*Zea mays* L.), soybean (*Glycine max* (L.) Merr.), rice (*Oryza sativa* L.), and wheat (*Triticum aestivum*)). The study found productivity gains for wheat under the ssp5.85 emission scenario, linked to higher concentrations of CO_2. Generally, highest gains under that emission scenario were found at higher latitudes beyond 50° N and under 30° S for all crops. Climate projections inherit a high degree of variability and uncertainty, especially with regard to precipitation distribution and climate extremes (Iles et al. 2020; Lhotka and Kyselý 2022; Sillmann et al. 2017; Semenov 2023). This is why climate modelers emphasize using a multi-model ensemble to include a wide range of possible projections (Tegegne et al. 2020; Wang et al. 2018; Hey et al. 2025). Given the structural differences of commonly used agro-hydrological models, it is also recommended to apply more than one model when evaluating agricultural management strategies (Gavasso-Rita et al. 2024; Turek et al. 2025). However, using an ensemble of climate and crop models, Rosenzweig et al. (2014) showed that the crop models might introduce a larger uncertainty than the climate models. A similar approach has been taken by Schewe et al. (2014) and Dams et al. (2015) where hydrological models were combined with global climate models and climate change scenarios in order to evaluate the impact of climate change on water scarcity and runoff, respectively. While the uncertainty of the climate model projections and, in particular, precipitation, is visible rather in terms of magnitude, the translation of precipitation to hydrological variables (soil moisture, runoff, etc.)

depends on regional properties (vegetation and soil properties), as well as how this is handled within the hydrological models (Schewe et al. 2014). However, besides the uncertainty added by a model ensemble, multi-model agreement indicated negative impacts on target parameters, such as the yield reduction of major crops in many agricultural regions at higher levels of warming (Rosenzweig et al. 2014).

The model inter-comparison presented by Jägermeyr et al. (2021) provided protocols for several setups (e.g., growing period and fertilizer inputs), yet did not consider homogenized soil tillage across models, which was identified as a weakness since the soil parameters affected by tillage influence soil hydrology and, consequently, crop growth (Müller et al. 2017; Müller et al. 2019). Given the importance and extent of wheat production in Europe (34% of the global wheat production), we explicitly aimed to test whether no-till can offset negative climate-change impacts on wheat yields. To do this, we examined how downscaled CMIP6 climate projections affect long-term (2020–2090) wheat production and whether replacing conventional tillage with no-till can serve as an effective adaptation strategy to counteract projected yield losses. To this end, we applied an ensemble of four agro-hydrological models driven by the above-mentioned future climates from six global climate models, focusing on the extent to which no-till provides adaptation benefits under future conditions at three sites along a north–south European gradient. The agro-hydrological models were calibrated and validated with data from long-term experiments in Denmark, Switzerland, and Austria that compare conventional tillage and no-till under crop residue removal. Using a suite of climate projection scenarios, we assessed whether no-till can mitigate adverse climate impacts by improving yield development and soil hydrological conditions.

2 | Material and Methods

2.1 | Model Descriptions

This study involved four agro-hydrological models, and each model was set up on and parameterized for all three LTEs (Section 2.2). The models' crop growth and hydrology modules are briefly presented below. All four models require information on weather, management, and soil as input data. Weather input includes daily measurements of temperature, precipitation, and global radiation. For the management simulated in this study, the input required includes the dates of sowing, fertilization, and tillage operations, the kind and quantity of fertilizer applied, as well as the tillage depth.

2.1.1 | APEX

2.1.1.1 | Crop Growth. The APEX (Agricultural Policy/Environmental eXtender) model is a field-scale agro-hydrological model that simulates crop growth and water, nitrogen (N), and carbon (C) dynamics in the vadose zone given an area with homogeneous climate, soil, landscape, crop rotation, and management system parameters. APEX is a continuous, physically based, spatially explicit model that runs on a daily time step (Izaurralde et al. 2006). It can simulate several crops, each of which has unique values for model parameters (Williams et al. 2023). The model accounts for crop rotations and field management practices, including cover crops, tillage, fertilizer types, mixed plant stands, and plant-weed competition (Wang et al. 2012). The seeding date of each crop is user defined and is an input into the model. The harvest date is model determined when the plant accumulated heat units match the potential heat units required to achieve maturity (Williams et al. 2023). The maximum potential daily plant growth and crop yields are limited by various environmental factors, including limitations caused by the availability of soil nitrogen, phosphorus, water, and aeration (Williams et al. 2023).

2.1.1.2 | Hydrology. The APEX model is physically based and simulates the hydrological components at the field scale of interception, infiltration, lateral flow, percolation, surface runoff, potential evapotranspiration (ET_p), actual evapotranspiration (ET_a), and snowmelt (Wang et al. 2012). The surface runoff volumes and peak runoff rates are empirically determined using a modification of the Soil Conservation Service (SCS) Curve Number (CN) method with a variable daily CN. In this study, the APEX model uses Richard's equation to simulate unsaturated water flow in the soil. The vertical flow component through the soil contributes to groundwater storage and can lead to deep percolation or return flow (Williams et al. 2023).

2.1.1.3 | Tillage. The model has several different tillage operations to choose from (Williams et al. 2023). For each tillage, the user specifies the depth of the tillage operation. The tillage function simulates changes in plant residue mixing into the soil (based on a mixing efficiency from 0 to 1). The tillage mixing equation is

$$X = \frac{(1.0 - EF) \cdot X_0 + EF \cdot SMX_0 \cdot (Z) - Z(l-1)}{TLD}, \quad (1)$$

where X is the amount of the material ($\mathrm{kg\,ha^{-1}}$) in a soil layer after mixing, EF is the mixing efficiency of the tillage operation (0–1), X_0 is the amount of the material ($\mathrm{kg\,ha^{-1}}$) before mixing, SMX_0 is the sum of the material in TLD before mixing ($\mathrm{kg\,ha^{-1}}$), Z is the depth (m) to the bottom of the plow layer, and TLD is the tillage depth (m). A fraction of the plant residuals (1.0 – EF) in the tillage depth is not mixed and the remaining material (EF) is mixed and distributed uniformly within the tillage depth.

The change in bulk density in the plough layer is simulated as follows:

$$\rho_p = \rho_{p0} - \left(\rho_{p0} - 0.667 \cdot \rho_b\right) \cdot EF \quad (2)$$

where ρ_p is the bulk density after tillage ($\mathrm{g\,cm^{-3}}$), ρ_{p0} is the bulk density in the soil layer before tillage ($\mathrm{g\,cm^{-3}}$), and ρ_b is the bulk density of the soil when it has completely settled after tillage ($\mathrm{g\,cm^{-3}}$). Between tillage operations, the soil settles with each rainfall event according to the inflow rate of water into the soil layer and the percentage of sand in the layer. Tillage operations also mix nutrients into the soil, and convert standing residues to flat residues. Other functions include simulating ridge height and surface roughness of the soil (Williams et al. 2023).

2.1.2 | CANDY

2.1.2.1 | Crop Growth. The original version of CANDY (CArbon and Nitrogen DYnamics) as presented first by Franko et al. (1995) focused primarily on simulating soil temperature, water content, and nitrogen dynamics. Since then, significant adaptations have been made, among others related to the crop growth module. Meanwhile, there are five plant modules available: CANDY_S (fixed N uptake for each crop type), CANDY_T (N uptake driven by transpiration), ZALF_ZF (biomass prediction for catch crop only), CDYGRN (grassland, grazing included), AGRO1 (generic plant development model). Regardless of the module that is being chosen, the crop state is always represented by four crop variables (crop height, root depth, soil coverage, N uptake). In this study, we used the generic plant module AGRO1, which is mainly based on the description of the AGRO-C model presented by Huang et al. (2009). The module is described in Turek et al. (2025). The model itself and related documentation can be found at https://www.somod.info/candy_main.php.

2.1.2.2 | Hydrology. CANDY describes water flux processes in the unsaturated zone using calculation layers of 10 cm depth. Lateral flux is not considered by the model. Surface runoff occurs if the amount of water in the upper layers is higher than the soil's pore volume, that is, when infiltration is no longer possible. Downward flow is described by the bucket model, that is, it is only possible if water storage exceeds the layer's field capacity. The velocity of the downward flow is driven by the saturated hydraulic conductivity (K_s) and through a drainage parameter (λ_p) (Glugla 1969; Koitzsch and Günther 1990). This parameter is calculated internally from K_s and the difference between pore volume (PV) and water content at field capacity. In cases where information about water content are not available, λ_p and K_s can be calculated based on information on the soil texture and the fraction of elutriable soil (see https://www.somod.info/CANDY22_MODEL.pdf for more information on the equations).

Different from the other models, the potential evapotranspiration (ET_p) in CANDY is calculated as follows:

$$ET_p = (1 + 0.004 \cdot h) \cdot E_p, \tag{3}$$

with h = crop height (cm) and E_p = pan evaporation (mm d^{-1}), calculated as $0.0041 \cdot (T_{air} + 22.7) \cdot (G + 2.09)$ where T_{air} = air temperature (°C) and G = daily global radiation (MJ m^{-2}). Further, the PET of intercepted water by the crop (EI_p) is calculated as $1.3 \cdot E_p$.

2.1.2.3 | Tillage. Besides averaging of the state variables for water, temperature, nitrogen, and all organic compounds over the indicated tillage depth, tillage further influences the bulk density. In the model, this is described as follows:

$$\rho_{new} = \rho_{old} - l \cdot \left(\rho_{old} - \frac{2}{3} \cdot \rho_0\right), \tag{4}$$

where ρ_{new}, ρ_{old}, and ρ_0 are the new, the old and completely re-compacted bulk densities (g cm^{-3}), respectively, and l is the loosening efficiency of the soil tillage tool [0–1]. l is user-specific and was kept at the default value of 0.7.

The bulk density after re-compaction (ρ_0) is calculated following an approach of (Ruehlmann and Körschens 2009) depending on the actual SOC content (%) at each time step:

$$\rho_0 = (2.631 + 15.811 \cdot b) \cdot e^{(b \cdot SOC)}, \tag{5}$$

where b is determined site-specifically during model initialization using the initially provided values for ρ_b and SOC. In case no initial value for ρ_b is provided, b is calculated as

$$b = \frac{(1.78345 - 0.0081 \cdot cl) - 2.684}{140.943}, \tag{6}$$

with cl representing the clay content (%).

2.1.3 | DAISY

2.1.3.1 | Crop Growth. Daisy is a crop model that simulates water, nitrogen, carbon, and pesticides in agricultural fields. The model does not only simulate processes in the soil, but ranges from the top of the canopy to the bottom of the root zone. The model simulates water flow in the soil, solute flow, soil organic matter turnover, soil vegetation atmosphere transfer (SVAT), and is integrated with a crop model, where a wide variety of crops and management practices are integrated, as well as a simpler generic plant growth model. The original version is described by Hansen et al. (1990) and Petersen et al. (1995) and generalized by Hansen and Abrahamsen (2009). The canopy structure is defined by a predefined leaf density distribution that varies with height, which depends on the development stage and leaf area index (LAI), where LAI depends on leaf mass and development stage. Partitioning, leaf and root death, senescence, and nitrogen stress (stress factors) are all influenced by development stage. Maintenance respiration depends on the dry mass of the plant components and on temperature.

2.1.3.2 | Hydrology. The hydrological component of Daisy is formulated as a one-dimensional, vertically resolved water balance model, driven by meteorological inputs and crop characteristics. The soil profile is discretized into user-defined layers, within which unsaturated water flow is simulated using the Richards equation. Soil hydraulic properties are parameterized using the van Genuchten–Mualem functions. The upper boundary conditions are defined by precipitation, irrigation, and potential evapotranspiration (calculated via the Hargreaves approach), with surface runoff estimated when infiltration capacity is exceeded. Root water uptake is modeled following a distributed extraction function dependent on root density and water stress, and is linked to plant transpiration demand. Numerical integration is performed using an implicit finite difference scheme to ensure stability under variable time steps. This hydrological module is fully coupled with Daisy's nitrogen transport and crop growth sub-models, allowing for simultaneous simulation of soil moisture dynamics, solute leaching, and plant–soil–atmosphere interactions over multiple seasons.

2.1.3.3 | Tillage. DAISY models tillage as a combination of mixing and translocation (Hansen et al. 1990). In general, the different soil layers are swapped, meaning that the soil layers that are above the ploughing depth will become inverted.

TABLE 1 | Mean (standard deviation; $n = 4$) soil texture at CENTS Flakkebjerg.

Soil depth (cm)	Treatment	Sand (%)	Silt (%)	Clay (%)	SOC ($mg\,C\,g\,soil^{-1}$)	Bulk density ($g\,cm^{-3}$)
10	CT	79.1 (3.1)	8.6 (1.4)	12.4 (2.0)	12.1 (0.6)	1.49 (0.03)
	NT	79.0 (4.2)	8.0 (2.3)	13.0 (2.3)	13.7 (1.6)	1.48 (0.10)
30	CT	78.9 (3.7)	8.6 (2.0)	12.5 (2.4)	9.1 (1.6)	1.60 (0.04)
	NT	75.7 (7.8)	9.2 (3.3)	15.1 (4.5)	8.1 (1.4)	1.59 (0.07)
50	CT	82.5 (8.2)	5.6 (2.0)	11.9 (6.2)	3.1 (1.0)	1.53 (0.03)
	NT	79.0 (7.8)	6.6 (2.8)	14.5 (5.6)	3.9 (0.3)	1.52 (0.04)

Note: Clay < 2 μm; silt 2–63 μm; sand 63–2000 μm.
Abbreviations: CT = conventional tillage with straw removal; NT = no-tillage with straw removal.

This *swap* action averages the temperature, water, nitrogen, SOM, pesticides, and other substances in these soil layers, but each soil layer maintains its bulk density. However, for rotavation, harrowing, seed bed preparation, and stubble cultivation, the soil layers above the working depth are mixed and the soil contents, as well as the bulk densities, are averaged.

2.1.4 | SWAP

2.1.4.1 | Crop Growth. For a dynamic representation of crop growth, SWAP (Soil Water Atmosphere Plant, Kroes et al. (2017)) implements the generic crop growth module WOFOST (WOrld FOod STudies) (de Wit et al. 2019), in which the absorbed radiation is a function of solar radiation and crop leaf area. The module allows describing plant physiological processes that determine the oxygen demand of plant roots.

2.1.4.2 | Hydrology. SWAP is a 1-D vertically directed agro-hydrological model that simulates the transport of water, solutes, and heat in the zone between the groundwater and the top of the plant canopy in variably saturated soils. In interaction with the crop development, the model simulates the heat and solute transport dynamics of variably saturated soils by employing the Richards equation (Richards 1931) in the vertical direction, including a sink term for root water uptake. Evapotranspiration and its separation between evaporation and transpiration were calculated based on the reference evapotranspiration in combination with crop factors. Surface runoff occurs when the rainfall rate exceeds the infiltration rate of the soil. The model does not consider hysteresis, preferential flow, drainage systems, solute transport, snow and frost, as well as neither salinity nor nutrient stress. The bottom boundary condition of the soil profile is defined according to field conditions, being free drainage the option used for deep freely draining soils. Runoff was calculated based on a constant threshold of 0.2 cm of water pounding, after which runoff occurs.

2.1.4.3 | Tillage. In SWAP, tillage was represented by assigning different soil hydraulic and structural properties to each tillage treatment, following practices used in SWAP tillage chronosequence and hydraulic-variability studies (e.g., Rodrigues Pinheiro and Nunes 2023). In contrast to the other three models, tillage is not represented as a single event but as long term effects reflected in the difference in soil hydraulic properties.

2.2 | Long-Term Field Experimental Data

This study used data from three European LTEs, namely CENTS (Denmark—DK), FAST I (Switzerland—CH), and Hollabrunn (Austria—AT). The sites represent different pedo-climatic conditions found in typical European agricultural farmland. The selected LTEs and their management histories are briefly described here—a more detailed description of the sites can be found in Holzkämper et al. (2024). Due to the complex field crop rotation management, it was decided that for the modelling setup, only the years in which winter wheat was grown without a cover crop should be used for model calibration and validation.

2.2.1 | CENTS

The experiment was established in 2002 on a sandy loam soil at the Flakkebjerg campus of Aarhus University (55°19′ N, 11°23′ E, 32 masl), Denmark (Hansen et al. 2010). The soil is based on ground morainic deposits from the last glaciation and is classified as a Glossic Phaeozem (Krogh and Greve 1999). The average soil organic carbon (SOC) content at the start of the experiment (2002) was 12 $mg\,g^{-1}$ (Hansen et al. 2015). The long-term average annual temperature and precipitation are 8.9°C and 581 mm, respectively. CENTS has a full-factorial randomized block design with four blocks (each block was 3 m wide and 40 m long) and four treatments (measuring 12.5 by 2.5 m, with a net area of each sub-subplot of 10.0 by 1.5 m), namely conventional tillage with straw removal in a crop rotation, conventional tillage with straw retention in a crop rotation, no-tillage with straw removal in a crop rotation, and no-tillage with straw retention in a crop rotation. In this study, the treatments with crop residue removal were used in the simulation experiment. The soil characteristics can be found in Table 1.

2.2.2 | FAST I

The FAST I field trial is located in Rümlang, close to Zürich, Switzerland (47° 43′ N, 8° 52′ E) at 485 m above sea level. It was started in 2009 to evaluate the performance of organic compared to conventional farming on production and ecosystem services (Wittwer et al. 2021). The climate is classified as humid continental with warm summers (Köppen classification: Dfb). The long-term average annual temperature and precipitation are 9.7°C and 1063 mm, respectively (climate period 1991–2020).

The soil has been classified as a calceric Cambisol with a loam texture (23% clay, 34% silt, 43% sand, USDA texture classification) and an average gravimetric organic carbon content of 1.4% in the topsoil. The crop rotation includes 2 years of ley as well as grain maize, spring pea (*Lathyrus vernus* (L.) Bernh.), and winter wheat. FAST I has a full-factorial randomized block design with four blocks and four treatments, namely conventional tillage with mineral fertilizer, conventional tillage with organic fertilizer, no-till with mineral fertilizer, and no-till with organic fertilizer. Each block consists of four plots (6 × 30 m), which again are subdivided into four quarters, of which two include cover crops and two do not (split-plot design). In this study, only the treatments with conventional tillage (CIT) and no-till (CNT) that had mineral fertilization and no cover crops were considered (Table 2).

2.2.3 | HOLL

The LTE Hollabrunn (HOLL) was started in 2006 and is located in Lower Austria, at the Agricultural School Hollabrunn, in north eastern Austria (48° 34′ N, 16° 5′ E; 248 m above sea level). The climate is temperate continental with a mean annual temperature of 10.2°C and a mean annual precipitation of 517 mm (GeoSphere Austria 2023). The soil is classified as chernozem (IUSS Working Group WRB 2015) with predominantly loamy silt texture (Table 3). The crop rotation at the LTE includes winter wheat, durum wheat, spring barley, and maize as cereals, as well as sugar beet, sunflower. A winter cover crop of a legume mix is applied. In 2021, soybeans were introduced into the rotation. The field experimental site is laid out in a complete randomized block design with three blocks (6 m × 50 m), each with four treatments. The two treatments examined in the study are inversion tillage (ITS) with incorporation of crop residues and no-till (NTS), that is, direct seeding with crop residues left on the field.

2.3 | Climate Projection Data

Future climate scenarios are downscaled CMIP6 scenarios for all three LTEs, using six global climate models (GCMs), namely CMCC-ESM2, CNRM-CM6-1, GISS-E2-1-G, HadGEM3-GC31-LL, MRI-ESM2-0, and UKESM1-0-LL. The downscaling was undertaken using the stochastic LARS-Weather Generator (LARS-WG v8, Semenov (2023)), which was "trained" on the observed period 1985–2015. Therefore, the LARS-WG baseline represents the year 2000 (1985–2015). The temporal resolution of the projected climate data was daily. The future simulation period was 2020–2090 with the first harvest taking place in 2021. For each GCM, the two emission scenarios (Shared Socioeconomic Pathways—ssps) ssp2-4.5 and ssp5-8.5 were selected with 50 realizations each. The ssp scenarios are a set of five narratives that describe the possible future development of human society to 2100 and describe different demographics, technologies, and economics and how these affect greenhouse gas (GHG) emissions and climate change mitigation (Shukla et al. 2022). The two contrasting ssps used is this study were chosen to span a large range of potential climate change impacts. While ssp2 represents a narrative reflecting more or less current global conditions, ssp5 is the narrative that represents the highest level of GHG

TABLE 2 | Mean (standard deviation; $n = 3$) soil texture and soil organic carbon (SOC) at FAST I.

Soil depth (cm)	Treatment	Sand (%)	Silt (%)	Clay (%)	SOC (mg C g soil^{-1})	Bulk Density (g cm^{-3})
10	CIT	43.9 (2.9)	35.6 (4)	20.5 (2.3)	13.6 (1)	1.31 (0.07)
	CNT	42.7 (3.4)	34.7 (4.5)	22.5 (2.5)	12.8 (2.6)	1.40 (0.03)
30	CIT	42.9 (6.3)	33.9 (4.4)	23.1 (2)	7.6 (2.5)	1.49 (0.05)
	CNT	43.9 (9.1)	32.7 (6.3)	23.5 (3.5)	6.8 (0.3)	1.48 (0.07)
50	CIT	45.7 (13)	34.1 (8)	20.2 (8.3)	5.1 (0.8)	1.51 (0.11)
	CNT	43.7 (14.7)	32.3 (8.1)	23.9 (8.1)	4.1 (0.2)	1.58 (0.04)

Note: Clay < 2 μm; silt 2–63 μm; sand 63–2000 μm.
Abbreviations: CIT = conventionally tilled with mineral fertilization and no cover crops; CNT = no-till with mineral fertilization and no cover crops.

TABLE 3 | Mean (standard deviation; $n = 4$) soil texture and soil organic carbon (SOC) at Hollabrunn, Austria.

Soil depth (cm)	Treatment	Sand (%)	Silt (%)	Clay (%)	SOC (mg C g soil^{-1})	Bulk density (g cm^{-3})
10	ITS	20.7 (0.67)	57.7 (1.60)	21.6 (1.50)	13.5 (0.83)	1.42 (0.09)
	NTS	20.8 (0.46)	57.3 (2.73)	21.9 (3.18)	13.9 (1.10)	1.59 (0.05)
30	ITS	19.5 (0.23)	58.3 (1.55)	22.2 (1.51)	11.3 (0.16)	1.51 (0.15)
	NTS	20.9 (1.78)	59.7 (4.82)	19.5 (4.65)	9.97 (0.76)	1.52 (0.14)
50	ITS	20.3 (2.50)	58.7 (3.46)	21.0 (3.19)	8.75 (1.74)	1.34 (0.08)
	NTS	16.3 (0.53)	63.6 (1.21)	20.1 (1.54)	7.37 (0.85)	1.32 (0.10)

Note: Clay < 2 μm; silt 2–63 μm; sand 63–2000 μm.
Abbreviations: ITS = inversion tillage with crop residue incorporation. NTS = no-till with direct seeding and residues left in the field.

emissions. The ssp2-4.5 is widely considered to be the "business-as-usual" scenario with an additional effective radiative forcing of $4.5\,W\,m^{-2}$ reaching the Earth's surface by the year 2100. In contrast, ssp5-8.5 is the "Fossil-fueled development" scenario with an additional effective radiative forcing of $8.5\,W\,m^{-2}$, which would lead to a median global warming of 4.2 C relative to the period 1850–1900 (Riahi et al. 2017; Chen et al. 2021). Thus, future climate simulations for each site consisted of 2 (ssps) × 6 (GCMs) × 50 (realizations) = 600 simulations of 71 years.

We used the Standardized Precipitation Index (SPI) (McKee et al. 1993; Keyantash and Dracup 2002) to identify drought conditions at the temporal scale for both the observed and projected climate using

$$\mathrm{SPI} = \frac{P - P^*}{\sigma_P} \tag{7}$$

with P = precipitation, P^* = mean precipitation, and σ_P = standard deviation of precipitation.

2.4 | Simulation Experiments

All four models were set up on the three LTEs (CENTS, FAST I, and HOLL) using a homogenized methodology. The workflow of the simulation experiments is shown in Figure S1.

2.4.1 | Soil Parametrization

In order to determine the effect of soil and crop management on soil physical, hydraulic, and mechanical properties, we used data on disturbed and undisturbed soil samples taken at 10, 30, and 50 cm soil depth at each LTE. For a detailed description of the determined parameters, see Heller et al. (2025) and Holzkämper et al. (2024). The field data used in this study includes soil organic carbon, the water retention, hydraulic conductivity, texture, and bulk density. This data was used during both the model calibration and the future projections. The estimated water retention and conductivity curves for CENTS, FAST I, and HOLL are shown in Figure 1.

2.4.2 | Model Calibration

Given that the focus of the study was on winter wheat, only the years in which winter wheat was grown in the crop rotation were used for the calibration and validation of the models. Subsequently, only the plant-related parameters were considered in the calibration process (Table S1).

Calibration was carried out on conventional treatments, that is, on the conventional and inversion tillage, respectively. In all simulations, straw or crop residues were removed after harvest. The validation of the models was carried out on the no-till (NT) treatments on each LTE. The number of years used for the calibration were 18 years for CENTS (8 years with winter wheat), 12 years for FAST I (5 years with winter wheat), and 15 years for HOLL (5 years with winter wheat). Also, as none of the LTEs included a winter wheat monoculture in their cropping systems, we assumed in the calibration that winter wheat was cultivated every year, but calibrated only on the years in which winter wheat was actually present in the rotation. For APEX, the calibration at HOLL using this method did not provide satisfactory results, hence the model was calibrated on Block B and validated on Blocks A and C.

To include the spatial heterogeneity of the individual sites, yields were calibrated across blocks. This means that the result of the calibration was one set of calibrated plant-related parameters per LTE, which best described the yield across the blocks. For CENTS, all four Blocks (A–D) were included. For FAST I, Block A was excluded due to the systematic significant difference in the observed crop yields, leaving three Blocks (B–D) for calibration, validation, and future scenarios. For HOLL, all three Blocks (A–C) were included.

The description of the soil profile in the models was based on Heller et al. (2025) and Holzkämper et al. (2024) (see Section 2.4.1). Given the sampling depths of 10, 30, and 50 cm, the models were set up with layers covering depths of 0–20, 20–40, and 40–120 cm. The maximum soil profile and rooting depths were set to 120 cm at each LTE. Management strategies, that is, sowing and harvesting, tillage operations and fertilizer applications were set in the models according to the information provided by the respective LTE. To calculate the potential evapotranspiration (ET_p), APEX, DAISY and SWAP used the Hargreaves equation. The equation used by CANDY to calculate ET_p are described in Equation 3.

2.4.3 | Model Evaluation

The root mean square error (RMSE) was used to assess the goodness-of-fit for the simulation results compared to the field data during calibration and validation:

$$\mathrm{RMSE} = \sqrt{\frac{1}{N}\sum_{i=1}^{N}\left(O_i - S_i\right)^2} \tag{8}$$

with N is the number of observations, O_i are the individual grain yield observations, and S_i are the simulated grain yields.

2.4.4 | Future Projections

For future scenarios (2020–2090), that is, using the climate projection data (see Section 2.3), a monocrop setup with winter wheat was simulated and the sowing date was fixed to 3rd October for CENTS (DK), 22nd October for FAST I (CH) and 27th October for HOLL (AT) (Table 4). The harvest dates were not considered fixed, but simulated by each model according to when the simulated maturity of the crop was reached. An average fertilizer application (date, amount, and type), as well as tillage (type, depth and times) were provided for each LTE and per treatment (Table 4).

In the case of SWAP, no fertilization was prescribed, meaning that the model was run with no nutrient stress. Further, the models did not consider increasing CO_2 concentrations in the atmosphere for the future periods, that is, the CO_2 fertilization sub-module, if existing in models, was turned off.

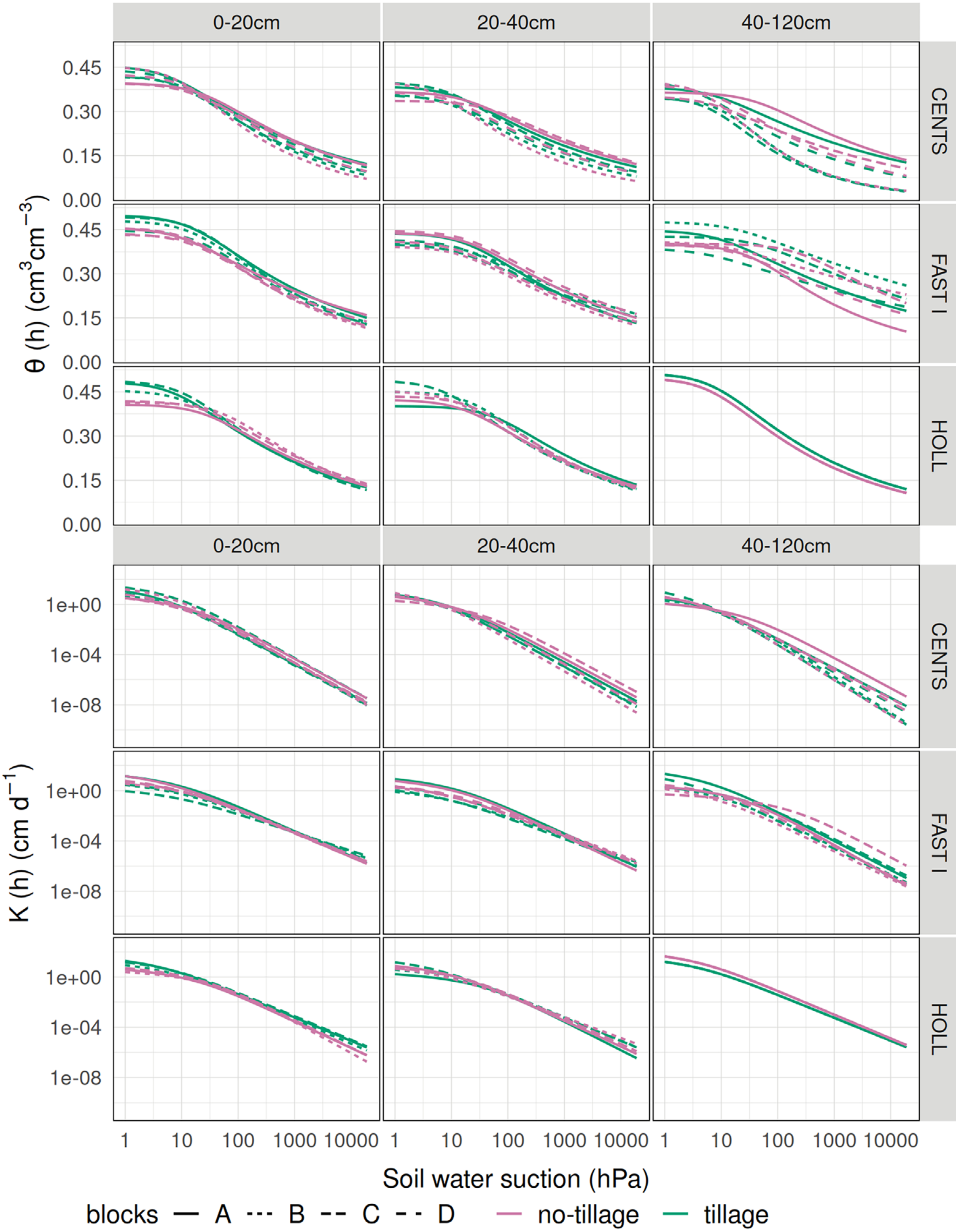

FIGURE 1 | Soil water retention and conductivity at average soil depths of 10, 30, and 50 cm under conventional tillage and no-till at CENTS (DK), FAST I (CH), and HOLL (AT). The multiple lines within each depth indicate the different blocks per site.

3 | Results

3.1 | Climate Projections

The projected annual precipitation and average annual temperature are shown in Figure S2. For all three sites, average air temperatures were projected to increase compared to the baseline (1985–2015) (Figure 2). Over all climate models, MRI-ESM2-0 under ssp2-4.5 projected the lowest increase in annual temperature for all three sites, while projections were highest under UKESM1-0-LL ssp5-8.5. For the Danish site, CENTS, temperature increases were between 1.1°C and 3.0°C for the ssp2-4.5 scenarios and between 1.7°C and 4.2°C for the ssp5-8.5 scenarios. For the Swiss site, FAST I, projected temperature changes ranged from 1.3°C to 3.8°C (ssp2-4.5) and 2.4°C to 5.3°C (ssp5-8.5), respectively. The highest increases

TABLE 4 | Management practices for continuous winter wheat at CENTS (DK), FAST I (CH), and HOLL (AT) implemented in the future scenario simulations.

Management	CENTS	FAST I	HOLL
Sowing date	3rd Oct	22nd Oct	27th Oct
Harvest date		Dynamic and model-dependent	
Mineral fertilizer application	3rd Apr (70 kg N ha^{-1})	22nd Mar (60 kg N ha^{-1})	12th Mar (50 kg N ha^{-1})
		29th Apr (30 kg N ha^{-1})	25th Apr (50 kg N ha^{-1})
		27th May (30 kg N ha^{-1})	22th May (37 kg N ha^{-1})
Manure application	23rd May (260 kg ha^{-1} as pig manure, which corresponds to 100 kg N ha^{-1})	—	—
Ploughing date and depth	2nd Oct (20 cm)	30th Sep (20 cm) and 19th Oct (10 cm)	19th Oct (25 cm)

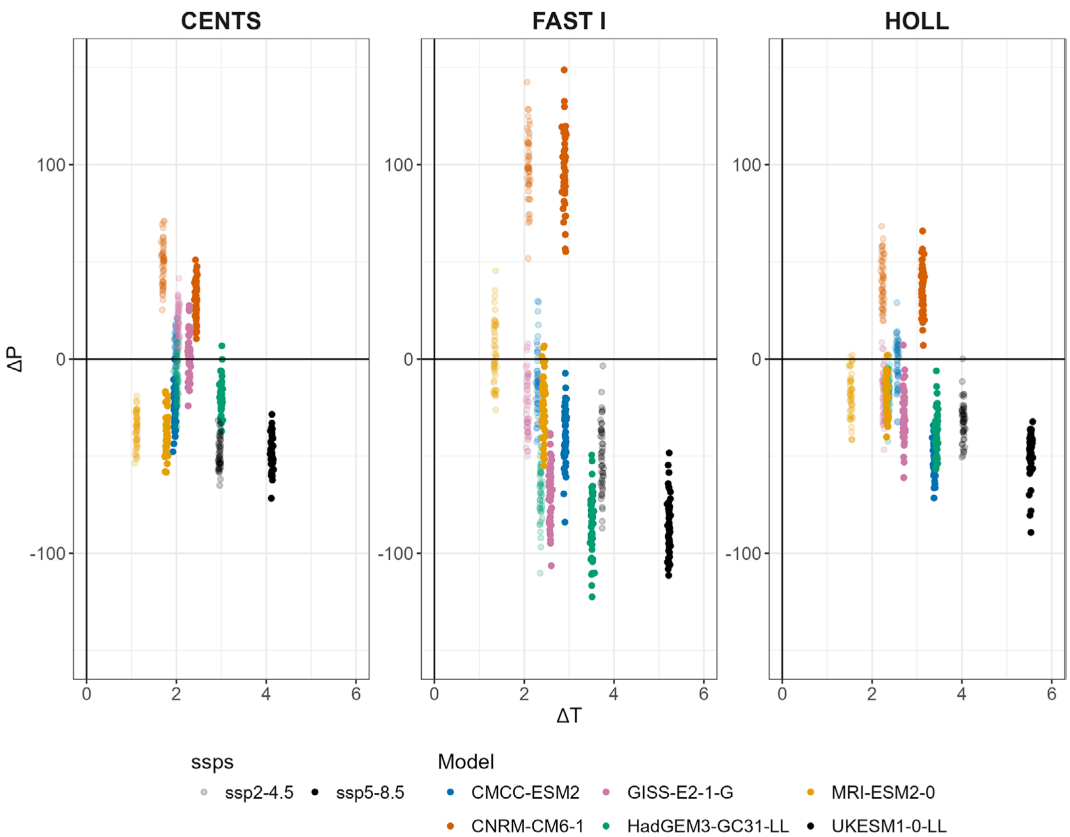

FIGURE 2 | Deviation of projected annual temperature (Δ*T*, °C) and precipitation (Δ*P*, mm) in mm from baseline weather data (1985–2015) for CENTS (DK), FAST I (CH), and HOLL (AT). Each climate model comes with 50 representations and two emission scenarios (ssp2-4.5 and ssp5-8.5).

were projected for the Austrian site, HOLL, with 1.5°C–4.1°C (ssp2-4.5) and 2.3°C and 5.6°C (ssp5-8.5), respectively. The projected changes in annual precipitation varied between the GCMs and each of them showed a wide range across the 50 representations (Figure 2). For each of the sites, depending on the GCM, the projected changes were positive (more precipitation) or negative (less precipitation) and for some GCMs, projected changes indicated both effects across the 50 representations. For CENTS, which has an average annual precipitation of about 579 mm (1985–2015), changes in projected annual precipitation were between −11% and +12% (−65.06 and 70.99 mm) under ssp2-4.5 and −12% and +9% (−71.70 and 50.97 mm) under ssp5-8.5. For both emission scenarios, the GCM UKESM1-0-LL predicted the highest decreases in precipitation, that is, years with drier conditions, while CNRM-CM6-1 predicted the highest increases, that is, years with wetter conditions. The highest increases and decreases in precipitation were projected for FAST I, that is, the site with the highest annual precipitation amounts used in this study (1026 mm over the 1985–2015 period). For this site, the highest decreases were projected by

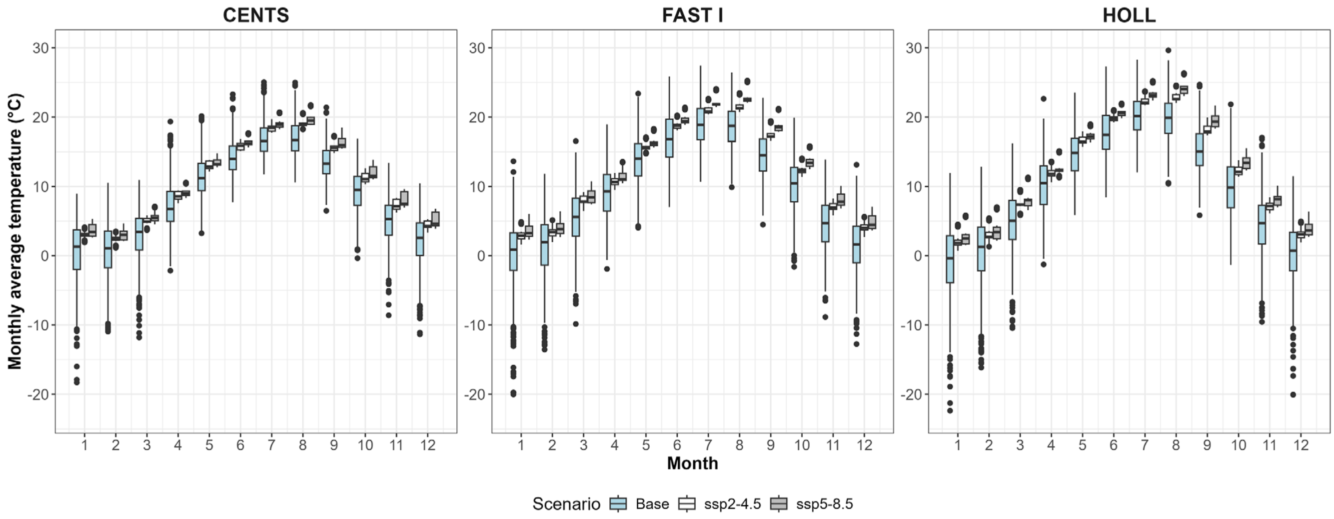

FIGURE 3 | Monthly average temperature at CENTS (DK), FAST I (CH), and HOLL (AT) for the baseline period (1985–2015), and two shared socio-economic pathways, ssp2-4.5 and ssp5-8.5.

HadGEM3-GC31-LL for both ssp2-4.5 (−11%; −110.24 mm) and ssp5-8.5 (−12%; −122.40 mm). Highest increases were projected by CNRM-CM6-1 ranging up to 14% (142.42 mm; ssp2-4.5) and 15% (148.80 mm; ssp5-8.5), respectively. Similar to CENTS, for HOLL, the two GCMs UKESM1-0-LL and CNRM-CM6-1 predicted the highest and lowest changes in annual precipitation, with CNRM-CM6-1 predicting wetter conditions independent of the emission scenario. Projections for HOLL, which is the driest if the three sites used in this study with an average annual precipitation amount of 512 mm, ranged from −10% (−50.53 mm) to +13% (68.20 mm) under ssp2-4.5 and −17% (−89.29 mm) to +13% (65.84 mm) under ssp5-8.5.

Even though projected average annual temperatures were above the baseline temperature, the range of monthly average temperatures was narrower both towards negative and positive temperatures (Figure 3). The climate models differed only slightly in projected monthly average temperatures, and even if temperatures were slightly higher under ssp5-8.5 in most months, this difference was rather minor.

In addition to the variation in annual precipitation totals, the distribution of precipitation and dry periods differed among the GCMs. On a monthly basis, the SPI for the three sites under the baseline scenarios, that is, 1985–2015, is mostly between −1 and 1, which means in the "neutral" range, and this is very consistent throughout the year (Figure S3). In contrast to that, the climate projections show a clear dynamic across the year with more distinct wet and dry periods. However, the projections differ in the timing of these rather extreme conditions (Figures S4–S9). For example, for CENTS, UKESM1-0-LL and CMCC-ESM2 predict wetter conditions during winter and spring, followed by drier conditions in summer and autumn. MRI-ESM2-0 predicts the opposite and spring is projected to be the driest period on average for all three sites. HadGEM3-GC31-LL predicts drier conditions in winter and wet conditions in late spring and early summer for CENTS and FAST I. For HOLL, conditions are rather neutral throughout the year under ssp2-4.5, but tend toward drier conditions in autumn and winter under ssp5-8.5. These variations in dry and wet conditions can be expected to influence winter wheat simulations, as weather conditions strongly determine the development and success of the crop.

TABLE 5 | Root mean squared errors (RMSEs) for the conventional treatments, that is, (inversion) tillage and straw removal.

Model	CENTS (DK)	FAST I (CH)	HOLL (AT)
APEX	1.1	0.7	1.3
CANDY	0.7	1.3	1.2
DAISY	1.6	1.3	1.5
SWAP	1.5	1.5	1.2

Note: Models were calibrated based on observed grain yield ($t\,ha^{-1}$).

3.2 | Model Calibration to Observed Grain Yield

Grain yields observed at the individual LTEs were in a similar order of magnitude. They varied across years but did not differ significantly between treatments (Figure S10). At CENTS, grain yields varied between 2.8–9.1 and 1.6–9.9 $t\,ha^{-1}$ under conventional tillage and no-till, respectively. The wide range is mainly due to the increase in yields after 2013, which occurred under both conventional tillage and no-till. At FAST I, yields under conventional tillage ranged from 4 to 6.3 $t\,ha^{-1}$ and from 3.1 to 6.2 $t\,ha^{-1}$ under no-till. However, over time, no clear increase or decrease in productivity was observed. The same applied to HOLL, where observed grain yields were between 5.4 and 8.3 $t\,ha^{-1}$ under conventional tillage and between 5 and 7.8 $t\,ha^{-1}$ under no-till.

The four models performed well in reproducing the winter wheat grain field observed at the three LTEs. For CENTS, RMSEs were between 0.7 (CANDY) and 1.6 $t\,ha^{-1}$ (DAISY) (Table 5). Similar results were achieved for FAST I, with RMSEs ranging from 0.7 (APEX) to 1.5 $t\,ha^{-1}$ (SWAP). For HOLL, model performances were even more similar, with RMSEs ranging from 1.2 (CANDY) to 1.5 $t\,ha^{-1}$ (DAISY). The calibrated crop parameters for each model and LTE can be found in Table S1.

3.3 | Simulation of Future Grain Yield

Given the large number of simulations and factors considered, we present block-averaged outcomes in the main text, as spatial heterogeneity among blocks had only minor effects relative to the influence of the climate projections. Full block-level results are provided in the Supporting Information.

No clear treatment effect was visible in the individual model simulations of the different blocks or among projections (Figures 4 and S11). Even though the average grain yields simulated by each model are in a comparable range at the individual LTEs, the models differ in both the trend and variability under the future climates.

APEX simulated a decreasing trend of grain yield over the simulation period for all sites and blocks and regardless of the management practice or climate projection. However, the yield variability caused by the different climate models was higher under tillage, at least at the CENTS and HOLL sites. At the CENTS site, CANDY simulated an initial decrease in yields until 2030, but after that, yields slightly increased. Under the ssp2-4.5 scenario, the yields more or less stabilize until 2090 for all climate projections except UKESM1-0-LL, where a slight downward trend is discernible. This trend becomes even stronger under the ssp5-8.5 scenario and is also visible under HadGEM3-GC31-LL and even CNRM-CM6-1. Yields simulated with DAISY show an increasing trend over time with slightly higher average yields under no-till compared to the tillage treatment. This increase is independent of the climate scenario, block, or management practice (Figures 4 and S11). Overall, the variation of the simulations was lower under no-till. SWAP simulated no significant trend in grain yield over the years, but the variation between climate projections was very high. The effect of tillage or no-till, which in SWAP is expressed by the difference in soil properties, did not result in a visible difference in grain yield.

For the FAST I site, CANDY simulated a slight increase in grain yields in the beginning and a yield decrease after 2060, where no clear treatment effects could be detected. The trends are somewhat similar to the ones at CENTS with decreasing yields towards the end of the simulation period under

FIGURE 4 | Climate projection results of winter wheat grain yield at CENTS (DK), FAST I (CH), and HOLL (AT) averaged across blocks. Full lines represent the median value between the climate projections, and the shaded area refers to the values between the (dotted) minimum and maximum values. Results shown are without an average moving window.

UKESM1-0-LL (both ssp2-4.5 and ssp5-8.5) and HadGEM3-GC31-LL (ssp5-8.5). While DAISY did not show much of a yield trend for any of the projections or treatments, APEX and SWAP simulated a somewhat decreasing trend over the 2020–2090 time period, independent of the climate scenario, GCM, or management. This decrease was stronger under the ssp5-8.5 scenario and particularly pronounced under the UKESM1-0-LL projection.

At the HOLL site, APEX simulated slightly decreasing yields over time, independent of the climate projection. Candy simulated a high variability in crop yields under no-till with a generally higher tendency towards lower yields. Overall, yields seem less stable under no-till compared to tillage, in particular under the ssp5-8.5 scenario. In contrast to that, DAISY simulated increasing yields over time and this was independent of the block, scenario, GCM, and treatment (Figure S11). SWAP simulated rather unstable yields across all GCMs, with no-till resulting in slightly lower yields on average. Surprisingly, SWAP simulated decreasing yield trends towards the end of the simulation period already under ssp2-4.5 under all GCMs but CMCC-ESM2. Under ssp5-8.5, conditions under GCMs CMCC-ESM2 and CNRM-CM6-1 obviously favored yields simulated with SWAP visible through an increasing trend over time.

In general, at all sites, SWAP simulated the highest variability in future yields. This variability can be linked to the variation in the runs within each climate model. This is particularly the case for the CENTS and HOLL sites, where the variation in simulated yields with SWAP was about twice as high as for the other models. This was independent of the climate model, climate scenario or block. The lowest variation in yields following climate models was found by CANDY, at least for CENTS and FAST I. At the HOLL site, DAISY simulated less variation in grain yields across the climate models. When averaging over the blocks, it becomes clear that the impact of the individual climate models and scenarios on simulated yield strongly differed between the models (Figure 4). While the climate projections under the ssp2-4.5 scenario did not cause much yield differences among climate models, stronger reactions by all four models are visible under ssp5-8.5. However, this reaction is different between the sites and climate model. Strongest yield decreases were simulated for the UKESM1-0-LL climate model, which also projects the highest increase in average temperature combined with the highest reduction in annual rainfall compared with the other climate models. However, at the HOLL site, CANDY and DAISY simulated increasing or steady yields for most of the climate models and regardless of the scenario or block (Figure S11). For this site, CANDY simulated tillage as beneficial to yield production compared to no-till and yields even decrease (temporarily) under no-till. No clear management effects are simulated by the other models.

3.4 | Simulation of Future Growing Period

The length of the growing period (days from sowing until harvest) was simulated by CANDY, DAISY, and SWAP (Figure 5). Regardless of the site, climate scenario, block, or management, all models simulated a gradual rather than abrupt trend towards a shorter growing period over the 2020–2090 period with no clear management effect (Figures 5 and S12).

While the trends among the models and differences between climate projections were similar among models, CANDY appeared to be the most sensitive of the three models and simulated the strongest decrease in the growing period. Compared to that, DAISY showed a more intermediate behavior, simulating clearly present declines that, however, were less steep than simulated by CANDY. SWAP showed comparatively mild reductions in growing period and some rather flat trends.

The strongest change in growing period was simulated for CENTS (particularly by CANDY), while the slopes were more moderate at FAST I and weakest for HOLL.

Under ssp2-4.5, CANDY simulated on average the strongest decrease in growing days (30, 29, and 24 days for CENTS, FAST I, and HOLL, respectively), resulting in the crop harvest being shifted from the end of July (24th July for CENTS, 22nd of July for FAST I, and 20th July for HOLL) to the end of June (24th, 23rd, and 26th of June for CENTS, FAST I, and HOLL, respectively). For DAISY, the length of the growing period decreased by 17, 16, and 15 days at CENTS, FAST I, and HOLL, respectively, but was generally longer as simulated by CANDY. At the end of the simulation period, harvest had been moved from 3rd August to 18th July at CENTS, 27th July to 11th July at FAST I, and from 17th July to 2nd July at HOLL. SWAP's simulated growing period was the least affected by the climate projections and harvest at the end of the growing period was simulated to occur around 17th of July instead of 30th of July at CENTS, 04th July instead of 18th of July at FAST I, and 11th July instead of 22nd of July at HOLL. Under spp5-8.5, the growing period decreased even more for all models, but most for CANDY (60, 55, and 49 days at CENTS, FAST I, and HOLL, respectively). Crop maturity and, consequently, harvest was thus simulated to happen around 25th May (CENTS), 27th May (FAST I), and 2nd June (HOLL), respectively. The simulated decrease in growing period was smaller for DAISY (27, 29, and 28 days at CENTS, FAST I, and HOLL, respectively) and SWAP (23 days at CENTS, 24 days at FAST I, and 22 days at HOLL). Consequently, crops simulated with DAISY and SWAP reached maturity much later compared to Candy, resulting in harvest dates around 7th July (CENTS), 28th June (FAST I), and 20th June (HOLL) with DAISY, and 7th July (CENTS), 23rd June (FAST I), and 1st July (HOLL) with SWAP.

The climate projections that resulted in the strongest decrease in growing period were CMCC-ESM2 and UKESM1-0-LL under the ssp2-4.5 scenario and UKESM1-0-LL under the ssp5-8.5 scenario.

Overall, the shortening of the growing period in all three models was mainly driven by the predicted climate with no recognizable treatment effects (Figure S12). The only exceptions are for SWAP at FAST I and HOLL, with 1 day difference between tillage and no-till (13 days under tillage vs. 14 days under no-till at FAST I and 22 days under tillage vs. 21 days under no-till at HOLL). The general lack of a treatment effect can be explained by the fact that simulating the crop phenology by the models

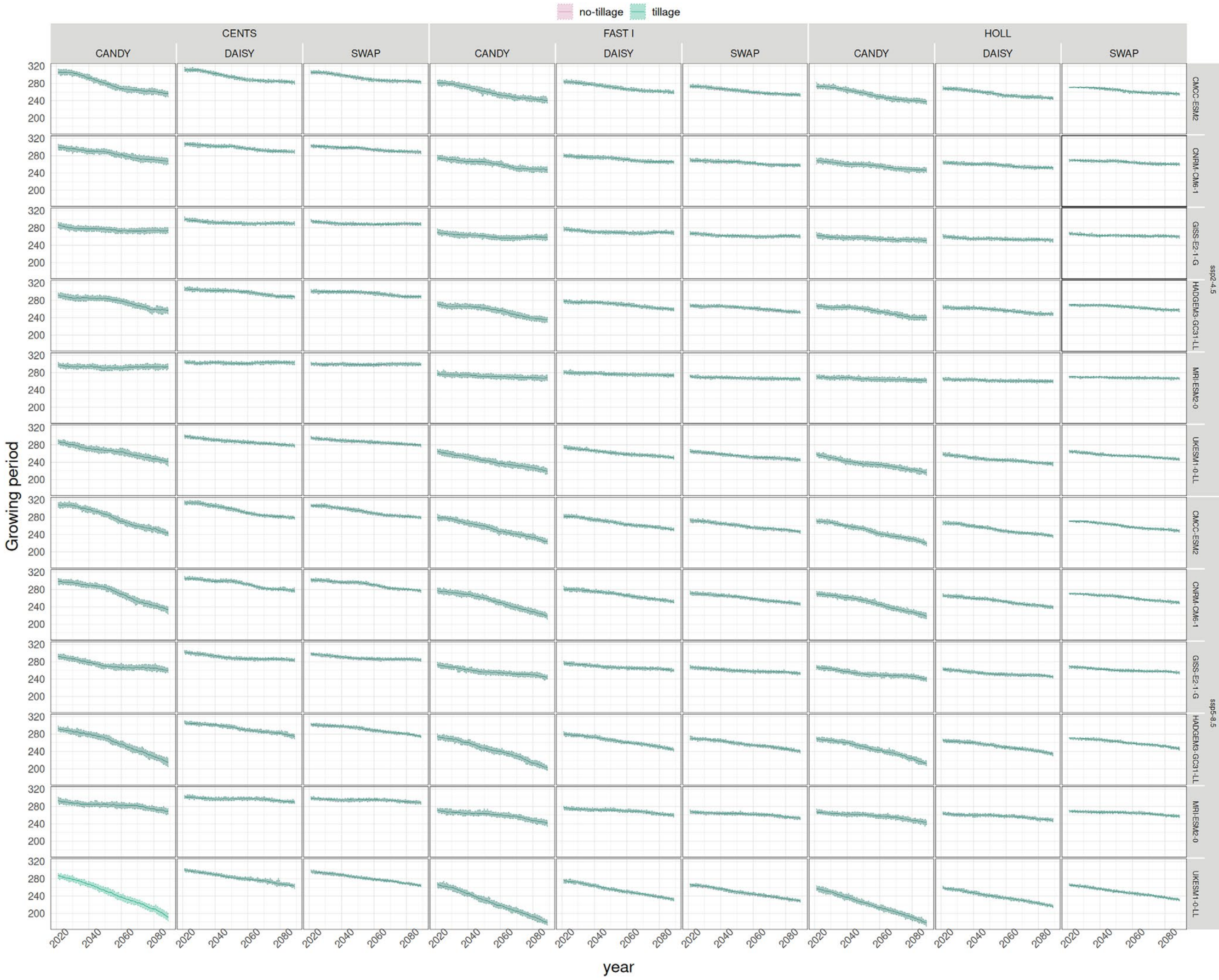

FIGURE 5 | Simulated growing period (days) at CENTS (DK), FAST I (CH), and HOLL (AT) averaged across blocks. Full lines represent the median value between the climate projections, and the shaded area refers to the values between the (dotted) minimum and maximum values. Results shown are without an average moving window.

is not connected to the soil, but is based on the growing degree days.

3.5 | Simulation of Future Water Balance Components

3.5.1 | Actual Evapotranspiration

At CENTS, APEX simulated decreasing ET_a over time with an average higher (but not significantly different) ET_a under tillage for all blocks and GCMs, ssp2-4.5 and ssp5-8.5 (Figures S13 and S14). CANDY, DAISY, and SWAP simulated no significant trend in average ET_a, and no differences between tillage and no-till were simulated. Under HadGEM3-GC31-LL and UKESM1-0-LL, DAISY simulated a slight increase in ET_a towards the end of the simulation period, as well as increasing variation after 2060.

At the FAST I site, SWAP showed no trend in ET_a, except for under UKESM1-0-LL where ET_a decreased over time. For all GCMs, average ET_a was slightly higher under no-till compared to tillage. CANDY and DAISY simulated very slight increases in ET_a for each block and GCM with no difference between managements. SWAP showed no trend in ET_a under ssp2-4.5, but a tendency towards a decreasing ET_a under ssp5-8.5 with no differences between tillage and no-till.

For HOLL, APEX simulated lower ET_a under no-till for all GCMs. The variation of simulated ET_a was very high and differences were not significant. The other three models did not simulate clear trends in ET_a, except for under UKESM1-0-LL, where UKESM1-0-LL decreased over time. No advantage of tillage or no-till was simulated.

3.5.2 | Percolation Amounts

At the CENTS site, all models simulated an increase in percolation, that is, the water flow below the lower boundary set at 120 cm soil depth, over time under CNRM-CM6-1 (ssp5-8.5) (Figures S15 and S16). While APEX simulated no-till to lead to higher percolation on average, CANDY simulated the opposite and percolation was always lower under no-till compared to tillage. While there was no differences between blocks for APEX, the management differences simulated by CANDY were inverted in Block B, that is, no-till led to slightly higher percolation. This effect was, however, not as pronounced as in Blocks A, C, and D (Figure S16). In general, CANDY simulated rather low percolation compared to the other models. No treatment differences were simulated by DAISY and SWAP. Under ssp5-8.5, CANDY, DAISY and SWAP indicated a decrease in percolation over time under HadGem3-GC31-LL and UKESM1-0-LL, regardless of the block. No other trends were simulated for this site.

Simulations for FAST I did not show any treatment effects by any of the models, except for CANDY who simulated a slightly higher average percolation in Block C (Figure S15). APEX simulated an increase in percolation or no trend at all, except for GISS-E2-1-G (ssp5-8.5), where the initial increase turned to a decrease after approximately half of the simulation period. For DAISY and SWAP, the variation across climate models was very high and the simulated percolation ranged between 15 and 115 $cm\,yr^{-1}$. These two models also simulated the strongest decrease in percolation under GISS-E2-1-G, HadGem3-GC31-LL, and MRI-ESM2-0.

For HOLL, highest percolation amounts were simulated by APEX, together with a decreasing trend over time for almost all GCMs and blocks. In contrast to that, the remaining three models simulated rather low percolation with no identifiable trend across GCMs and blocks (Figure 16). However, throughout the simulations, APEX indicated higher percolation under no-till compared to tillage.

3.5.3 | Surface Runoff

Regardless of the site, block or GCM, DAISY and SWAP simulated surface runoff that was (close to) zero, except for SWAP at FAST I in Block C (Figures S17 and S18). As clearly seen by the high percolation amounts simulated by both models, the low runoff can be explained by the fact that almost all the water infiltrated into the soil. In contrast to this, APEX and CANDY simulated surface runoff at all sites, in all blocks and for all GCMs.

At CENTS, APEX simulated no clear trends and no differences in runoff between tillage practices. Simulated percolation increased a little over time under CNMR-CM6-1 (ssp5-8.5) and decreased under HadGem3-GC31-LL and UKESM1-0-LL. While CANDY did not simulate any clear trends either, the simulation results indicated a treatment effect with higher runoff under no-till in Blocks A, C, and D, while runoff under tillage was close to zero. This was the opposite in Block B, where CANDY simulated slightly higher runoff under tillage and almost no runoff at all under no-till. The variation in simulated runoff was higher under no-till than under tillage.

For FAST I, APEX and CANDY showed some variation in runoff over time, but no visible trend under ssp2-4.5. Even though the variation across climate models was similar between the models, average runoff simulated with CANDY was approximately twice as high as with APEX. Under ssp5-4.5, both APEX and CANDY simulated decreasing runoff over time. No clear treatment differences were visible, even though maximum runoff simulated with CANDY was higher under tillage compared to no-till. However, this treatment effect was limited to Blocks B and C (Figure S18).

At HOLL, APEX did not indicate any treatment effects regardless of the block and climate scenario. CANDY simulated higher runoff under no-till compared to tillage for Blocks A and B. For Block C, simulated runoff was close to zero under tillage and only slightly higher under no-till.

4 | Discussion

4.1 | Projection of a Future Climate

The climate projections used in this study were derived from Lars-WG including six global climate models for two emission scenarios with 50 representations each. This climate model ensemble guaranteed a variation in predicted climate conditions, spanning from overall wetter years to significantly drier years. The variation among the 50 representations is reflected in the agro-hydrological models as well, as the processes described by them are usually very sensitive to meteorologic data. Thus, the choice of a climate model ensemble minimizes the bias that would be introduced by using only one single climate model (Hey et al. 2025). A common feature of the climate models was the predicted increase in annual temperature by at least 1°C at each site (Figure 2). Given the global thresholds of 1.5°C and 2°C, respectively, suggested by the Intergovernmental Panel on Climate Change (Shukla et al. 2022), it has to be stressed that only MRI-ESM2-0 predicted temperature increases below 1.5°C for all three sites, but only under the lower emission scenario (ssp2-4.5) (Figure 2). The other climate models and scenarios were closer to and mostly above the 2°C increase in annual average temperatures.

Following the IPCC's Sixth report (van Diemen et al. 2022), when a pattern of extreme weather persists for a longer time, for example, a season, it can be classified as extreme climate event. This relates to high temperatures, as well as drought and high rainfall. Climate change is expected to increase the probability and, at the same time, frequency of extreme events, such as drought. More specifically, the projected changes in drought strongly differ among regions, as well as in the type of drought (agricultural, meteorological, and hydrological) (Caretta et al. 2022). While not only precipitation patterns will change, higher evaporative demands and changes in snow cover are additional drivers of future drought events in many regions of the world (Naumann et al. 2018; Cook et al. 2020).

4.2 | Projection of Wheat Production Under a Future Climate

The model ensemble including four agro-hydrological models (APEX, CANDY, DAISY, and SWAP) was run with an ensemble of climate projections for three sites, located in Northern and Central Europe, respectively, in order to evaluate the impact of conventional and no-tillage on future grain yields for winter wheat, as well as selected properties of the soil water balance. It was expected that differences in soil hydraulic properties derived by management practices (tillage vs. no-till) will lead to differences in grain yield in the long-term. The reasoning behind this was that the mechanical disturbance of the soil through frequent tillage influences the soil structure, hydrology, and consequently, the buffer capacity of the soil against changes in climate. Overall, all six GCMs used in this study indicated drought events of different severity and at different times of the year. In general, drought conditions during the reproductive development of winter wheat can significantly reduce the yield (e.g., Mu et al. (2021)). However, the exact timing of the drought during crop development is important and based on results obtained by Mu et al. (2021), sufficient water supply should be ensured during jointing and filling periods. During these periods, water shortage can affect the number of grains per head, as well as the size of the grains. In addition to that, water stress during seedling and tillering can hinder germination and root development. Besides drought, increasing temperature, and consequently, a faster reach of the growing degree days needed for crop maturity will result in shorter growing periods. This has already been reported for Denmark, where increasing temperatures have negatively affected grain filling on winter wheat yield, due to a decrease in the length of the growing season (Kristensen et al. 2011). In the scenario simulations used in this study, winter wheat was sown on 3rd, 22nd, and 27th October at CENTS, FAST I, and HOLL, respectively. Most GCMs predicted rather neutral conditions during this period, following the SPI definition. Exceptions are UKESM1-0-LL and CMCC-ESM2 at HOLL, which indicated drier conditions. Very important for the development of winter wheat is when plants experience vernalization, that is, a period of low winter temperatures (usually close to or below 0°C). While winter temperatures below 0°C are very common at the three sites, projected monthly average temperatures were never below 0°C (Figure 3).

Across all four agro-hydrological models and simulation setups used in this study, no differences in grain yield were observed between the different management practices. The models did, however, react differently to the climate predictions and how future grain yields until 2090 would develop: APEX simulated decreasing winter wheat yields for all sites and management practices along the future period. On average, trends simulated by CANDY, DAISY, and SWAP were different between the sites and while yields were projected to slightly increase at the CENTS and HOLL sites, the models simulated a decrease or no changes for the FAST I site. However, the models reacted to the more severe climate models, that is, the ones that indicated the highest temperature increase and strongest reduction of precipitation among all climate models (HadGEM3-GC31-LL and UKESM1-0-LL; Figures S7 and S9). While differences exist between the models in terms of yield development, all models indicated a reduction in grain yields under UKESM1-0-LL and partially also HadGEM3-GC31-LL, which predicted most pronounced reductions in annual precipitation across the three sites (Figure 2). Nevertheless, the precipitation patterns of those two GCMs were very different, as indicated by the SPI (Figures S7 and S9): UKESM1-0-LL projected slightly wetter conditions during late winter and early spring and indicated drier summers and autumns independent of the emission scenario. In contrast to that, HadGEM3-GC31-LL predicted drier winters and somewhat wetter springs (at least for CENTS). Overall, the projected differences between the sites highlight the need for region- and season-specific risk assessment, as well as adaptation planning (Becker et al. 2025).

4.3 | Soil Parameters and Model Parameterization

Parts of the explanation for the missing response of the models to management practice might be the soil parameterization, that is, the measurements derived from the respective LTEs and blocks, respectively. All three LTEs compare conventional and conservational management practices, with a particular focus on tillage versus no-till. At CENTS, these two treatments are further combined with straw removal or straw retention. It was expected that the different treatment would lead to changes in the soil physical and soil hydraulic properties in the long-term. The CENTS has been operating for 22 years and FAST I for 15 years under the same management practices. Differences in soil hydraulic properties are, however, less pronounced than might have been expected. In fact, larger differences could be found between the blocks than between treatments. These differences were partially captured by the models. Since modelling approaches rely heavily on specific soil parameters to determine hydraulic properties, in situ measurements of how these properties vary in the field and between treatments are paramount to improve our understanding of water movement in unstable soils Assouline and Or (2013). SWAP was most sensitive to the differences in soil hydraulic parameters between treatments and blocks, respectively. Overall, if the models showed differences between blocks at all, it was mainly evident at the CENTS site. CENTS has, compared to FAST I, a very high sand content (> 70%) and a clay content between 12% and 18% in the 0–50 cm layer. Nevertheless, the bulk density (ρ_b) is rather high, and there are no significant differences between the tillage treatments along the sampled depth (down to 50 cm deep). The soil is particularly compacted below the plough layer and ρ_b at 30 cm soil depth averaged across all four blocks is $1.60 \pm 0.06\,\mathrm{Mg\,m^{-3}}$ for conventional and $1.59 \pm 0.07\,\mathrm{Mg\,m^{-3}}$ for no-till (Heller et al. 2025). Generally, low ρ_b is associated with favorable hydraulic properties for agricultural purposes. Tillage can reduce ρ_b, but a lower ρ_b caused by mechanical disturbance and soil inversion is not stable and does not remain low over the growing season. The study of Kool et al. (2019) showed that the largest change in ρ_b happened within the first few weeks after tillage and that changes were more pronounced with depth. Based on the data used in this study, the loosening effect of tillage was limited to the topsoil layer and ρ_b increased with depth below the plough layer in the tilled treatments. This is true for all three sites used in this study (CENTS, FAST I, and HOLL), even though there are some differences between the blocks. Kool et al. (2019) further showed that the increase in ρ_b strongly affected water retention: for the initial ρ_b of $0.94\,\mathrm{g\,cm^{-3}}$ a volumetric water content of $0.19\,\mathrm{cm^3\,cm^{-3}}$ at a suction (ψ) of 330 hPa indicated that water was retained in only about one third of the pore volume, while at a ρ_b of $1.31\,\mathrm{g\,cm^{-3}}$, the decrease in pore volume along with increased water retention resulted in water being retained in two thirds of the pore volume at a suction of 330 hPa. Of the two modeling approaches evaluated in their study for changes in water retention as a function of ρ_b, Kool et al. (2019) found that only the one approach that used a matching point gave reasonable results for the entire range, despite not accounting for the bimodal shape of the curve. The model for K_s required separate estimates for $\rho_b < 1.06\,\mathrm{g\,cm^{-3}}$, and $\rho_b > 1.06\,\mathrm{g\,cm^{-3}}$. The effect on K_s was not obvious for $\rho_b < 1.06\,\mathrm{g\,cm^{-3}}$, but for $\rho_b > 1.06\,\mathrm{g\,cm^{-3}}$, K_s decreased by an order of magnitude as ρ_b increased. These kind of results have implications for simulation approaches of tilled soils, as well as for studies comparing tilled and non-tilled soils, as obviously, hydraulic properties of tilled soils will vary strongly depending on the time since the last tillage operation and the soil depth. While the soil hydraulic parameters did not seem to have much influence on the grain yield, some differences were found for some components of the water balance (ET_a, percolation and surface runoff). CANDY reacted most pronounced to differences between the blocks and this was most visible for the runoff. At CENTS, runoff simulated with CANDY was significantly higher under no-till compared to tillage for Blocks A, C, and D. Runoff under tillage was low in these blocks. For Block B, it was the other way around, and CANDY simulated higher runoff under tillage compared to no-till. A comparison of soil parameters of Blocks A and B for the conventional and no-till treatments shows that both blocks had the same ρ_b in the topsoil under tillage (1.50 Mg m^{-3}) but substantial differences under no-till (1.55 Mg m^{-3} for Block A and 1.38 Mg m^{-3} for Block B). At 30 cm soil depth, bulk densities were higher under tillage (1.58 Mg m^{-3} for Block A and 1.64 Mg m^{-3} for Block B) compared to no-till (1.56 Mg m^{-3} for Block A and 1.53 Mg m^{-3} for Block B). Related to that, topsoil porosity in Block A was higher under tillage (46% under conventional compared to 40% under no-till). This was not the case in Block B were the porosity was higher under no-till (42% vs. 45%). Most pronounced differences between the two blocks and treatments were visible in the saturated hydraulic conductivity (K_s): in Block A, the continuous tillage led to a very high K_s of 145 cm d^{-1}, while this value was much lower under no-till (15 cm d^{-1}). For Block B, the opposite is true and no-till had a higher K_s compared to tillage (22 vs. 79 cm d^{-1}). In CANDY, which uses the bucket model concept to simulate downward flow in soil, runoff occurs as soon as the topsoil layer is saturated, the lower porosity in Block A most likely led to a slightly higher runoff under no-till. APEX, DAISY, and SWAP used the Richards equation and also here, runoff is simulated when topsoil is saturated. However, surface runoff simulated by DAISY and SWAP was very low, while APEX simulated surface runoff in the same order of magnitude as CANDY (Figures S16 and S17).

Besides the initially set bulk density, the management itself would normally be expected to change the soil structure and soil hydraulic parameters over time. CANDY includes soil loosening by tillage, but this effect was not strong enough to provide evidence of tillage or no-till as a climate adaptation measure. In general, tillage is represented in the models as the redistribution of water, temperature, nitrogen, and soil organic carbon over the tillage depth. In DAISY, this also applies to pesticides and other substances in the topsoil layer, and APEX further considers surface features such as ridge height and roughness. However, accurate prediction of the long-term effects of soil management practices, such as on crop yield trajectories, could benefit from explicit representation of tillage-induced soil disturbance in crop models. This includes alterations to soil structure and associated hydraulic properties, which in turn modulate crop growth and yield development over time, particularly under projected climate change scenarios. It would be expected that simulating dynamic soil properties, particular changes in soil hydraulic conductivity and water retention, would allow the models to better capture critical periods of water stress or excess that govern phenological transitions and resource capture. This would further strengthen the coupling between soil processes and crop physiology, which could lead to more reliable forecasts of yield variability under diverse management and changing climatic conditions.

The models considered in this study differ considerably in their sensitivities to soil parametrization. This has already been shown by Turek et al. (2025) who evaluated the sensitivity of the same set of models on soil hydraulic properties determined by different pedotransfer functions compared to the model structures. In that study, SWAP showed the strongest sensitivity to the pedotransfer functions used. In the study presented here, the differences in simulated outputs with SWAP were less driven by differences in soil properties, that is, the management or block, but rather by the climate model, as is the case for the other models as well.

4.4 | Limitations of the Study

A limitation of this study is the fact that not all models account for dynamics in soil hydraulic parameters. While some keep soil properties related to the soil water retention curve constant throughout the simulation period others incorporate some temporal variation. However, consideration of the temporal variation of soil properties is necessary to accurately predict long-term effects of both agricultural management and climate change on soil quality and future crop yields (e.g., Strudley et al. (2008)). Dynamics in soil structure are considered by the USSF (Uppsala model for soil structure and function) model (Jarvis et al. 2022, 2024). The model considers the dynamic interactions between abiotic factors, soil crop growth and root development and soil structural changes. For example, it does make a direct link between the soil water conditions, the mineralization rates of soil organic matter, and increases or decreases in soil bulk density (Meurer, Chenu, et al. 2020). By applying the USSF model to the FAST I site and using some of the climate scenarios used in the study presented here, Feifel (2024) found that no-till had a positive effect on the soil water balance, resulting in reduced surface runoff and a better preservation of the soil moisture compared to tillage. In their study, under increased temperatures during the climate scenarios, a shortened growth period resulted in a reduction in crop yields, as the period for grain filling is getting shorter. Nevertheless, no-till maintained higher soil organic matter stocks and conserved soil moisture, thus demonstrating a great potential to mitigate some of the adverse impacts of climate change Feifel (2024).

Considering the agricultural practices simulated, it was assumed in this study that the same practices would be repeated every year. That means that the sowing dates, as well as the manure and mineral fertilizer application would occur on the same days, year after year. Also the quantity of fertilizer applied was kept constant. Only the harvest date was determined by the models that was based on the maturity of the crop (phenology) by each model, respectively. It is very likely that management practices would be adapted over the future time-span considered in this study. In their study, Bracho-Mujica et al. (2024) found that the impacts of technological advances on future wheat and maize yields were stronger than those resulting from climate change. Furthermore, the practice of planting winter wheat as a monoculture year after year is rather unlikely, just like the continuous cropping with the same winter wheat cultivar and a fixed sowing date. Using the STICS model, Yang et al. (2019) found that using earlier flowering cultivars, as well as earlier sowing, were adaptation options that were able to reverse the yield reductions. However, this was chosen as a homogeneous setup for model comparison in the model ensemble. The wheat monocrop setup with fixed fertilizer levels has consequences for APEX in particular, as it led to a steady and constant depletion of soil mineral nitrogen in the root zone over the period 2020–2090, thus resulting in decreasing yields over time.

Also, increasing atmospheric CO_2 concentration was not considered. This has been pointed out as a very important source of uncertainty in future yield projection (Kersebaum and Nendel 2014), as yields have been shown to increase under increased CO_2 (Long et al. 2005; Wang et al. 2013). However, in their study comparing the models DAISY, FASSET, and SWAT, Ozturk et al. (2017) showed that simulated winter wheat yields decreased or did not change under a future climate, but that the decrease was less pronounced when increased CO_2 concentration was taken into account.

Besides these shortcomings, to the best of our knowledge, the combination of different models, different climate scenarios and the combination of no-till versus tillage has not been conducted before. Even though there is high uncertainty within the years and models, the mean of the ensemble shows clear trends (although high variability [Wallach et al. 2025]). Nevertheless, studies like ours might be of interest for plant breeders to predict phenotype from genotype more accurately and prioritize traits for selection. Crop models, if properly parameterized, can provide a way to evaluate managed stress environments and integrate them with multi-environment field trials (Diepenbrock et al. 2022). In that way, the importance of adaptation in management, for example, sowing date, to specific plant traits can be evaluated both under ambient and predicted future climates.

5 | Conclusions

In this multi-model study, we could not detect the hypothesized positive effect of no-till compared to tillage on winter wheat yield development and selected hydrological components at three long-term field experiments under future climate scenarios. However, depending on the site, the underlying soil hydraulic properties of the blocks, but in particular the differences introduced by the climate models were more decisive in the modeled output than the differences induced by management practices. In addition to that, the setup chosen in this study, that is, four models on three LTEs with different management practices and 50 realizations of the climate scenarios, resulted in a high variability in simulated results.

Nevertheless, our study found that the adaptation benefits of no-till on winter wheat productivity were minimal under both current and future climate conditions at the three sites. This indicates that adopting tillage or no-till does not necessarily lead to a reduction in grain yield, suggesting stability in production regardless of the approach chosen. No-till did, however, demonstrate positive effects on water balance components. In the long term, adapting more conservational soil management practices might offer additional environmental advantages—something that should be addressed in future studies and modelling work.

Even though the (temporal) development of soil degradation due to unsustainable management may be hard to capture in LTEs due to small experimental plots, it would play an important role in real fields. Consequently, more site-specific adaptation measures need to be established and besides soil management practices, advanced crop varieties and their resilience have to be considered, for example, through plant breeding breeding. In a next step, trends of SOC, as well as the fate of soil nitrogen (e.g., through N_2O emissions and/or leaching) will be taken into account. Further, additional sites in Central and Southern Europe will be included in the study, in order to be able to consider different initial states of the LTEs before simulating future climate scenarios.

Author Contributions

Katharina Hildegard Elisabeth Meurer: conceptualization, methodology, writing – original draft, writing – review and editing, visualization, data curation. **Maria Eliza Turek:** conceptualization, methodology, writing – review and editing, visualization, data curation. **Johannes Wilhelmus Maria Pullens:** conceptualization, methodology, writing – review and editing, data curation. **Edberto Moura-Lima:** conceptualization, methodology, writing – review and editing, data curation. **Jeroen D. M. Schreel:** methodology, writing – review and editing, data curation. **Annelie Holzkämper:** conceptualization, funding acquisition, methodology, project administration. **Bano Mehdi-Schulz:** conceptualization, methodology, writing – review and editing.

Acknowledgments

This project was developed in the framework of the SoilX project. SoilX is part of the European Joint Program for SOIL “Towards climate-smart sustainable management of agricultural soils” (EJP SOIL) funded by the European Union Horizon 2020 research and innovation programme (Grant Agreement No. 862695). The authors would like to thank Olivier Heller and Raphaël Wittwer for soil analysis and data provision.

Funding

This project was developed in the framework of the SoilX-EJP SOIL project, part of the European Joint Program SOIL “Towards climate smart sustainable management of agricultural soils” (EJP SOIL) funded by the European Union Horizon 2020 Research and Innovation Program (862695).

Conflicts of Interest

The authors declare no conflicts of interest.

Data Availability Statement

The data that support the findings of this study are available from the corresponding author upon reasonable request.

References

Asseng, S., F. Ewert, P. Martre, et al. 2015. “Rising Temperatures Reduce Global Wheat Production.” *Nature Climate Change* 5: 143–147. https://doi.org/10.1038/nclimate2470.

Assouline, S., and D. Or. 2013. "Conceptual and Parametric Representation of Soil Hydraulic Properties: A Review." *Vadose Zone Journal* 12: 1–20. https://doi.org/10.2136/vzj2013.07.0121.

Becker, R., B. Schauberger, R. Merz, S. Schulz, and C. Gornott. 2025. "The Vulnerability of Winter Wheat in Germany to Air Temperature, Precipitation or Compound Extremes Is Shaped by Soil-Climate Zones." *Agricultural and Forest Meteorology* 361: 110322. https://www.sciencedirect.com/science/article/pii/S0168192324004350.

Blanchy, G., G. Bragato, C. Di Bene, et al. 2023. "Soil and Crop Management Practices and the Water Regulation Functions of Soils: A Qualitative Synthesis of Meta-Analyses Relevant to European Agriculture." *Soil* 9: 1–20. https://soil.copernicus.org/articles/9/1/2023/.

Blanchy, G., T. D'Hose, C. Donmez, et al. 2024. "An Open-Source Metadataset of Running European Mid- and Long-Term Agricultural Field Experiments." *Soil Use and Management* 40: e12978. https://doi.org/10.1111/sum.12978.

Bracho-Mujica, G., R. P. Rötter, M. Haakana, et al. 2024. "Effects of Changes in Climatic Means, Variability, and Agro-Technologies on Future Wheat and Maize Yields at 10 Sites Across the Globe." *Agricultural and Forest Meteorology* 346: 109887. https://www.sciencedirect.com/science/article/pii/S0168192324000029.

Caretta, M. A., A. Mukherji, M. Arfanuzzaman, et al. 2022. "Water." In *Climate Change 2022: Impacts, Adaptation and Vulnerability. Contribution of Working Group II to the Sixth Assessment Report of the Intergovernmental Panel on Climate Change*, edited by H.-O. Pörtner, D. C. Roberts, M. Tignor, et al., 551–712. Cambridge University Press.

Chen, D., M. Rojas, B. Samset, et al. 2021. "Framing, Context, and Methods." In *Climate Change 2021: The Physical Science Basis. Contribution of Working Group I to the Sixth Assessment Report of the Intergovernmental Panel on Climate Change*. Cambridge University Press.

Cook, B. I., J. S. Mankin, K. Marvel, A. P. Williams, J. E. Smerdon, and K. J. Anchukaitis. 2020. "Twenty-First Century Drought Projections in the cmip6 Forcing Scenarios." *Earth's Future* 8: e2019EF001461. https://doi.org/10.1029/2019EF001461.

Dams, J., J. Nossent, T. Senbeta, P. Willems, and O. Batelaan. 2015. "Multi-Model Approach to Assess the Impact of Climate Change on Runoff." *Journal of Hydrology* 529: 1601–1616. https://www.sciencedirect.com/science/article/pii/S0022169415005958.

de Wit, A., H. Boogaard, D. Fumagalli, et al. 2019. "25 Years of the Wofost Cropping Systems Model." *Agricultural Systems* 168: 154–167. https://www.sciencedirect.com/science/article/pii/S0308521X17310107.

Diacono, M., and F. Montemurro. 2010. "Long-Term Effects of Organic Amendments on Soil Fertility. A Review." *Agronomy for Sustainable Development* 30: 401–422.

Diepenbrock, C. H., T. Tang, M. Jines, et al. 2022. "Can We Harness Digital Technologies and Physiology to Hasten Genetic Gain in Us Maize Breeding?" *Plant Physiology* 188: 1141–1157.

Duan, H., G. Zhang, S. Wang, and Y. Fan. 2019. "Robust Climate Change Research: A Review on Multi-Model Analysis." *Environmental Research Letters* 14: 033001.

Ewert, F., M. Rounsevell, I. Reginster, M. Metzger, and R. Leemans. 2005. "Future Scenarios of European Agricultural Land Use: I. Estimating Changes in Crop Productivity." *Agriculture, Ecosystems and Environment* 107: 101–116. https://www.sciencedirect.com/science/article/pii/S0167880904003627.

FAOSTAT. 2023. "Faostat." Accessed September 7, 2025. http://faostat.fao.org/site/567/default.aspx#ancor.

Feifel, M. 2024. "Soil Management for Sustainable Agriculture Under Climate Change. A Modelling Study." Master's thesis, Swedish University of Agricultural Sciences, Faculty of Natural Resources and Agricultural Sciences, Department of Soil and Environment, Soil and Environmental Physics, Uppsala, Sweden. https://stud.epsilon.slu.se/20619/1/feifel_m_20241025.pdf. Programme: EnvEuro - European Master in Environmental Science, Course coordinating dept: Department of Soil and Environment.

Franko, U., B. Oelschlägel, and S. Schenk. 1995. "Simulation of Temperature-, Water- and Nitrogen Dynamics Using the Model Candy." *Ecological Modelling* 81: 213–222.

Gavasso-Rita, Y. L., S. M. Papalexiou, Y. Li, A. Elshorbagy, Z. Li, and C. Schuster-Wallace. 2024. "Crop Models and Their Use in Assessing Crop Production and Food Security: A Review." *Food and Energy Security* 13: e503. https://doi.org/10.1002/fes3.503. E503 FES3-2023-03-0049.R1.

GeoSphere Austria. 2023. "2023 jahresbericht. Annual report, GeoSphere Austria – Bundesanstalt für Geologie, Geophysik, Klimatologie und Meteorologie, Hohe Warte 38, 1190 Wien, Austria." https://www.geosphere.at/de/themen/natuerliche-ressourcen/wasser-als-ressource/geosphere-austria-jahresbericht-2023-1.pdf. Concept and editorial: Clemens Porpaczy. Proofreading: Christian Cermak. Layout: https://www.macheiner.st. Translation: KERN Austria GmbH. Production: Datapress GmbH, Linz.

Glugla, G. 1969. "Berechnungsverfahren zur ermittlung des aktuellen wassergehalts und gravitationswasserabflusses im boden." *Archives of Agronomy and Soil Science* 13: 371–376.

Hansen, E., L. Munkholm, B. Melander, and J. Olesen. 2010. "Can Non-Inversion Tillage and Straw Retainment Reduce n Leaching in Cereal-Based Crop Rotations?" *Soil and Tillage Research* 109: 1–8. https://www.sciencedirect.com/science/article/pii/S0167198710000541.

Hansen, E. M., L. J. Munkholm, J. E. Olesen, and B. Melander. 2015. "Nitrate Leaching, Yields and Carbon Sequestration After Noninversion Tillage, Catch Crops, and Straw Retention." *Journal of Environmental Quality* 44: 868–881. https://doi.org/10.2134/jeq2014.11.0482.

Hansen, S., and P. Abrahamsen. 2009. *Modeling Water and Nitrogen Uptake Using a Single-Root Concept: Exemplified by the Use in the Daisy Model*, 169–195. CRC Press.

Hansen, S., H. E. Jensen, N. E. Nielsen, and H. Svendsen. 1990. "Daisy—Soil Plant Atmosphere System Model. *Tech. rep.*, Miljøstyrelsen. NPo-forskning fra Miljøstyrelsen, Strandgade 29, 1401 København K".

Heller, O., L. ten Damme, T. D'Hose, et al. 2025. "Dataset of Physical, Biological and Chemical Soil Properties From 10 European Long-Term Experiments (1.1). Data Set." https://doi.org/10.5281/zenodo.13988072.

Hey, L., K. H. Meurer, and H. F. Jungkunst. 2025. "On the Potential of Biogeochemical Models to Predict Hot Moments of n2o Following Dry-Wet Cycles." *Atmospheric Environment: X* 27: 100347. https://www.sciencedirect.com/science/article/pii/S2590162125000371.

Holland, J. 2004. "The Environmental Consequences of Adopting Conservation Tillage in Europe: Reviewing the Evidence." *Agriculture, Ecosystems and Environment* 103: 1–25. https://www.sciencedirect.com/science/article/pii/S0167880904000593.

Holzkämper, A., L. ten Damme, T. D'Hose, et al. 2024. "EJP SOIL-Soilx: Final Project Report." *Technical Report, Zenodo*. https://doi.org/10.5281/zenodo.14001120.

Huang, Y., Y. Yu, W. Zhang, et al. 2009. "Agro-c: A Biogeophysical Model for Simulating the Carbon Budget of Agroecosystems." *Agricultural and Forest Meteorology* 149: 106–129. https://www.sciencedirect.com/science/article/pii/S0168192308002062.

Iles, C. E., R. Vautard, J. Strachan, S. Joussaume, B. R. Eggen, and C. D. Hewitt. 2020. "The Benefits of Increasing Resolution in Global and Regional Climate Simulations for European Climate Extremes." *Geoscientific Model Development* 13: 5583–5607. https://gmd.copernicus.org/articles/13/5583/2020/.

IUSS Working Group WRB. 2015. *World Reference Base for Soil Resources 2014, Update 2015: International Soil Classification System for Naming Soils and Creating Legends for Soil Maps*, 203. FAO.

Izaurralde, R. C., J. R. Williams, W. B. McGill, N. J. Rosenberg, and M. C. Q. Jakas. 2006. "Simulating Soil c Dynamics With Epic: Model Description and Testing Against Long-Term Data." *Ecological Modelling* 192: 362–384.

Jägermeyr, J., C. Müller, A. C. Ruane, et al. 2021. "Climate Impacts on Global Agriculture Emerge Earlier in New Generation of Climate and Crop Models." *Nature Food* 2: 873–885.

Jarvis, N., E. Coucheney, E. Lewan, et al. 2024. "Interactions Between Soil Structure Dynamics, Hydrological Processes, and Organic Matter Cycling: A New Soil-Crop Model." *European Journal of Soil Science* 75: e13455. https://doi.org/10.1111/ejss.13455.

Jarvis, N., J. Groh, E. Lewan, et al. 2022. "Coupled Modelling of Hydrological Processes and Grassland Production in Two Contrasting Climates." *Hydrology and Earth System Sciences* 26: 2277–2299. https://hess.copernicus.org/articles/26/2277/2022/.

Kersebaum, K., and C. Nendel. 2014. "Site-Specific Impacts of Climate Change on Wheat Production Across Regions of Germany Using Different co2 Response Functions." *European Journal of Agronomy* 52: 22–32. https://www.sciencedirect.com/science/article/pii/S116103011300052X.

Keyantash, J., and J. A. Dracup. 2002. "The Quantification of Drought: An Evaluation of Drought Indices." *Bulletin of the American Meteorological Society* 83: 1167–1180.

Koitzsch, R., and R. Günther. 1990. "Modell zur ganzjährigen simulation der verdunstung und der bodenfeuchte landwirtschaftlicher nutzflächen mit und ohne bewuchs." *Archiv für Acker- Und Pflanzenbau Und Bodenkunde = Archives of Agronomy and Soil Science* 34: 803–810.

Kool, D., B. Tong, Z. Tian, J. Heitman, T. Sauer, and R. Horton. 2019. "Soil Water Retention and Hydraulic Conductivity Dynamics Following Tillage." *Soil and Tillage Research* 193: 95–100. https://www.sciencedirect.com/science/article/pii/S0167198718312212.

Kopittke, P., N. Menzies, P. Wang, B. McKenna, and E. Lombi. 2019. "Soil and the Intensification of Agriculture for Global Food Security." *Environment International* 132: 105078. https://doi.org/10.1016/j.envint.2019.105078.

Kristensen, K., K. Schelde, and J. E. Olesen. 2011. "Winter Wheat Yield Response to Climate Variability in Denmark." *Journal of Agricultural Science* 149: 33–47.

Kroes, J. G., J. C. van Dam, R. P. Bartholomeus, et al. 2017. "SWAP 4 - theory including user manual. *Tech. rep.*, Alterra, Wageningen University and Research." https://www.swap.alterra.nl/Documents/Kroes_etal_2017_SWAP_version_4_ESG_Report_2780.pdf. Technical Report.

Krogh, L., and M. Greve. 1999. "Evaluation of World Reference Base for Soil Resources and Fao Soil Map of the World Using Nationwide Grid Soil Data From Denmark." *Soil Use and Management* 15: 157–166. https://doi.org/10.1111/j.1475-2743.1999.tb00082.x.

Lhotka, O., and J. Kyselý. 2022. "Precipitation–Temperature Relationships Over Europe in Cordex Regional Climate Models." *International Journal of Climatology* 42: 4868–4880. https://doi.org/10.1002/joc.7508.

Long, S. P., E. A. Ainsworth, A. D. Leakey, and P. B. Morgan. 2005. "Global Food Insecurity. Treatment of Major Food Crops With Elevated Carbon Dioxide or Ozone Under Large-Scale Fully Open-Air Conditions Suggests Recent Models May Have Overestimated Future Yields." *Philosophical Transactions of the Royal Society, B: Biological Sciences* 360: 2011–2020.

McKee, T. B., N. J. Doesken, and J. Kleist. 1993. "The Relationship of Drought Frequency and Duration to Time Scales." In *Proceedings of the 8th Conference on Applied Climatology*, 179–183. American Meteorological Society.

Meurer, K., J. Barron, C. Chenu, et al. 2020. "A Framework for Modelling Soil Structure Dynamics Induced by Biological Activity." *Global Change Biology* 26: 5382–5403. https://doi.org/10.1111/gcb.15289.

Meurer, K. H. E., C. Chenu, E. Coucheney, et al. 2020. "Modelling Dynamic Interactions Between Soil Structure and the Storage and Turnover of Soil Organic Matter." *Biogeosciences* 17: 5025–5042. https://bg.copernicus.org/articles/17/5025/2020/.

Meurer, K. H., N. R. Haddaway, M. A. Bolinder, and T. Kätterer. 2018. "Tillage Intensity Affects Total Soc Stocks in Boreo-Temperate Regions Only in the Topsoil—A Systematic Review Using an Esm Approach." *Earth-Science Reviews* 177: 613–622. https://www.sciencedirect.com/science/article/pii/S0012825217305135.

Mu, Q., H. Cai, S. Sun, et al. 2021. "The Physiological Response of Winter Wheat Under Short-Term Drought Conditions and the Sensitivity of Different Indices to Soil Water Changes." *Agricultural Water Management* 243: 106475. https://www.sciencedirect.com/science/article/pii/S0378377420313275.

Müller, C., J. Elliott, J. Chryssanthacopoulos, et al. 2017. "Global Gridded Crop Model Evaluation: Benchmarking, Skills, Deficiencies and Implications." *Geoscientific Model Development* 10: 1403–1422. https://gmd.copernicus.org/articles/10/1403/2017/.

Müller, C., J. Elliott, D. Kelly, et al. 2019. "The Global Gridded Crop Model Intercomparison Phase 1 Simulation Dataset." *Scientific Data* 6: 50.

Naumann, G., L. Alfieri, K. Wyser, et al. 2018. "Global Changes in Drought Conditions Under Different Levels of Warming." *Geophysical Research Letters* 45: 3285–3296. https://doi.org/10.1002/2017GL076521.

Ogle, S. M., C. Alsaker, J. Baldock, et al. 2019. "Climate and Soil Characteristics Determine Where No-Till Management Can Store Carbon in Soils and Mitigate Greenhouse Gas Emissions." *Scientific Reports* 9: 11665.

Ozturk, I., B. Sharif, S. Baby, M. Jabloun, and J. E. Olesen. 2017. "The Long-Term Effect of Climate Change on Productivity of Winter Wheat in Denmark: A Scenario Analysis Using Three Crop Models." *Journal of Agricultural Science* 155: 733–750.

Pagliai, M., N. Vignozzi, and S. Pellegrini. 2004. "Soil Structure and the Effect of Management Practices." *Soil and Tillage Research* 79: 131–143. https://www.sciencedirect.com/science/article/pii/S0167198704001394.

Peixoto, D. S., L. C. M. D. Silva, L. B. B. Melo, et al. 2020. "Occasional Tillage in No-Tillage Systems: A Global Meta-Analysis." *Science of the Total Environment* 745: 140887.

Petersen, C., U. Jørgensen, H. Svendsen, S. Hansen, H. Jensen, and N. Nielsen. 1995. "Parameter Assessment for Simulation of Biomass Production and Nitrogen Uptake in Winter Rape." *European Journal of Agronomy* 4: 77–89. https://www.sciencedirect.com/science/article/pii/S1161030114800191.

Pittelkow, C. M., B. A. Linquist, M. E. Lundy, et al. 2015. "When Does No-Till Yield More? A Global Meta-Analysis." *Field Crops Research* 183: 156–168. https://www.sciencedirect.com/science/article/pii/S0378429015300228.

Riahi, K., D. van Vuuren, E. Kriegler, et al. 2017. "The Shared Socioeconomic Pathways and Their Energy, Land Use, and Greenhouse Gas Emissions Implications: An Overview." *Global Environmental Change* 42: 153–168. https://doi.org/10.1016/j.gloenvcha.2016.05.009.

Richards, L. 1931. "Capillary Conduction of Liquids Through Porous Mediums." *Physics* 1: 318–333.

Rodrigues Pinheiro, E. A., and M. R. Nunes. 2023. "Long-Term Agro-Hydrological Simulations of Soil Water Dynamic and Maize Yield in a Tillage Chronosequence Under Subtropical Climate Conditions." *Soil & Tillage Research* 229: 105654.

Rosenzweig, C., J. Elliott, D. Deryng, et al. 2014. "Assessing Agricultural Risks of Climate Change in the 21st Century in a Global Gridded Crop Model Intercomparison." *Proceedings of the National Academy of Sciences* 111: 3268–3273. https://doi.org/10.1073/pnas.1222463110.

Ruehlmann, J., and M. Körschens. 2009. "Calculating the Effect of Soil Organic Matter Concentration on Soil Bulk Density." *Soil Science Society of America Journal* 73, no. 3: 876–885.

Schewe, J., J. Heinke, D. Gerten, et al. 2014. "Multimodel Assessment of Water Scarcity Under Climate Change." *Proceedings of the National Academy of Sciences* 111: 3245–3250. https://doi.org/10.1073/pnas.1222460110.

Semenov, M. 2023. "LARS-WG Weather Generator." Accessed October 30, 2024. https://sites.google.com/view/lars-wg/.

Shukla, P. R., J. Skea, A. Reisinger, et al., eds. 2022. *Summary for Policymakers*. Cambridge University Press.

Sillmann, J., T. Thorarinsdottir, N. Keenlyside, et al. 2017. "Understanding, Modeling and Predicting Weather and Climate Extremes: Challenges and Opportunities." *Weather and Climate Extremes* 18: 65–74. https://www.sciencedirect.com/science/article/pii/S2212094717300440.

Six, J., E. Elliott, and K. Paustian. 2000. "Soil Macroaggregate Turnover and Microaggregate Formation: A Mechanism for c Sequestration Under No-Tillage Agriculture." *Soil Biology and Biochemistry* 32: 2099–2103. https://www.sciencedirect.com/science/article/pii/S0038071700001796.

Soane, B., B. Ball, J. Arvidsson, G. Basch, F. Moreno, and J. Roger-Estrade. 2012. "No-Till in Northern, Western and South-Western Europe: A Review of Problems and Opportunities for Crop Production and the Environment." *Soil & Tillage Research* 118: 66–87. https://doi.org/10.1016/j.still.2011.10.015.

Strudley, M. W., T. R. Green, and J. C. Ascough. 2008. "Tillage Effects on Soil Hydraulic Properties in Space and Time: State of the Science." *Soil and Tillage Research* 99: 4–48. https://www.sciencedirect.com/science/article/pii/S0167198708000196.

Tegegne, G., A. M. Melesse, and A. W. Worqlul. 2020. "Development of Multi-Model Ensemble Approach for Enhanced Assessment of Impacts of Climate Change on Climate Extremes." *Science of the Total Environment* 704: 135357. https://www.sciencedirect.com/science/article/pii/S0048969719353495.

Trnka, M., R. Rötter, M. Ruiz-Ramos, et al. 2014. "Adverse Weather Conditions for European Wheat Production Will Become More Frequent With Climate Change. *Nature*." *Climate Change* 4: 637–643. https://doi.org/10.1038/nclimate2242.

Turek, M. E., J. W. M. Pullens, K. H. E. Meurer, E. Moura Lima, B. Mehdi-Schulz, and A. Holzkämper. 2025. "Pedotransfer Functions Versus Model Structure: What Drives Variance in Agro-Hydrological Model Results?" *European Journal of Soil Science* 76: e70088. https://doi.org/10.1111/ejss.70088.

van Diemen, R., J. Matthews, V. Möller, et al. 2022. "Annex I: Glossary." In *Climate Change 2022: Mitigation of Climate Change. Contribution of Working Group III to the Sixth Assessment Report of the Intergovernmental Panel on Climate Change*, edited by P. R. Shukla, J. Skea, R. Slade, et al. Cambridge University Press.

Wallach, D., T. Palosuo, H. Mielenz, et al. 2025. "Why Is There So Much Variability in Crop Multi-Model Studies?" *Agricultural and Forest Meteorology* 372: 110697. https://www.sciencedirect.com/science/article/pii/S016819232500317X.

Wang, B., L. Zheng, D. L. Liu, F. Ji, A. Clark, and Q. Yu. 2018. "Using Multi-Model Ensembles of cmip5 Global Climate Models to Reproduce Observed Monthly Rainfall and Temperature With Machine Learning Methods in Australia." *International Journal of Climatology* 38: 4891–4902. https://doi.org/10.1002/joc.5705.

Wang, L., Z. Feng, and J. K. Schjoerring. 2013. "Effects of Elevated Atmospheric co2 on Physiology and Yield of Wheat (*triticum aestivum* l.): A Meta-Analytic Test of Current Hypotheses." *Agriculture, Ecosystems & Environment* 178: 57–63. https://www.sciencedirect.com/science/article/pii/S0167880913002181.

Wang, X., J. R. Williams, P. W. Gassman, et al. 2012. "Epic and Apex: Model Use, Calibration, and Validation." *Transactions of the ASABE* 55: 1447–1462.

Williams, J. R., R. C. Izaurralde, C. Williams, and E. M. Steglich. 2023. *Agricultural Policy/Environmental Extender Model: Theoretical Documentation, Version 1501*. Technical Report. U.S. Department of Agriculture.

Wittwer, R. A., S. F. Bender, K. Hartman, et al. 2021. "Organic and Conservation Agriculture Promote Ecosystem Multifunctionality." *Science Advances* 7: eabg6995. https://doi.org/10.1126/sciadv.abg6995.

Yang, C., H. Fraga, W. van Ieperen, H. Trindade, and J. A. Santos. 2019. "Effects of Climate Change and Adaptation Options on Winter Wheat Yield Under Rainfed Mediterranean Conditions in Southern Portugal." *Climatic Change* 154: 159–178. https://doi.org/10.1007/s10584-019-02419-4.

Supporting Information

Additional supporting information can be found online in the Supporting Information section. **Figure S1:** Work flow of simulation experiments used in this study. **Figure S2:** Annual precipitation and average annual temperature at the three sites (FL = Flakkebjerg- CENTS, HO = Hollabrunn- HOLL, RE = Reckenholz- FAST I) projected by six climate models with 50 representations under two emission scenarios. **Figure S3:** SPI values for the three sites under the baseline scenario, that is, 1985–2015. CENTS = DK, FAST I = CH, HOLL = AT. **Figure S4:** Monthly SPI following climate projections with CMCC-ESM2 for the period 2020–2090. **Figure S5:** Monthly SPI following climate projections with CNRM-CM6-1 for the period 2020–2090. **Figure S6:** Monthly SPI following climate projections with GISS-E2-1-G for the period 2020–2090. **Figure S7:** Monthly SPI following climate projections with HadGEM3-GC31-LL for the period 2020–2090. **Figure S8:** Monthly SPI following climate projections with MRI-ESM2-0 for the period 2020–2090. **Figure S9:** Monthly SPI following climate projections with UKESM1-0-LL for the period 2020–2090. **Figure S10:** Observedwinterwheatgrain yields ($t\,ha^{-1}$) under conventional tillage (black) and no-till (grey) at three long-term field experiments. Dot represent average yields and error bars represent standard deviation. CENTS-Denmark, FAST I- Switzerland, and HO. **Figure S11:** Simulated grain yield ($kg\,ha^{-1}$) with SHP measured at Blocks A, B, C, and D in CENTS (DK), FAST I (CH) and HOLL (AT) per climate model and scenario. Full lines represent the median value between the repetitions within each climate model and shaded area refers to the values between the (dotted) minimum and maximum values. Results shown are without an average moving window. Note that for FAST I, Block A was excluded from the analysis. The Austrian LTE, HOLL, consists of three Blocks only (A–C). **Figure S12:** Simulated growing period on CENTS (DK), FAST I (CH), and HOLL (AT) per block. Full lines represent the median value between the repetitions within each climate model. Shaded area refers to the values between the (dotted) minimum and maximum values. Results shown are without an average moving window. **Figure S13:** Simulated evapotranspiration (ET_a) on CENTS (DK), FAST I (CH) and HOLL (AT) per climate model and scenario. Full lines represent the median value between the repetitions within each climate model and the blocks of the experiments. Shaded area refers to the values between the (dotted) minimum and maximum values. Results shown are without an average moving window. **Figure S14:** Simulated evapotranspiration (ET_a) with SHP measured at Blocks A, B, C, and D in CENTS (DK), FAST I (CH) and HOLL (AT) per climate model and scenario. Full lines represent the median value between the repetitions within each climate model and shaded area refers to the values between the (dotted) minimum and maximum values. Results shown are without an average moving window. Note that for FAST I, Block A was excluded from the analysis. The Austrian LTE, HOLL, consists of three Blocks only (A–C). **Figure S15:** Simulated annual percolation amounts on CENTS (DK), FAST I (CH) and HOLL (AT) per climate model and scenario. Full lines represent the median value between the repetitions within each climate model and the blocks of the experiments. Shaded area refers to the values between the (dotted) minimum and maximum values. Results shown are without an average moving window. **Figure S16:** Simulated annual percolation amounts with SHP measured at Blocks A, B, C, and D in CENTS (DK), FAST I (CH) and HOLL (AT) per climate model and scenario. Full lines represent the median value between the repetitions within each climate model and shaded area refers to the values between the (dotted) minimum and maximum values. Results shown are without an average moving window. Note that for FAST I, Block A was excluded from the analysis. The Austrian LTE, HOLL, consists of three Blocks only (A–C). **Figure S17:** Simulated surface runoff on CENTS (DK), FAST I (CH) and HOLL (AT) per climate model and scenario. Full lines represent the median value between the repetitions within each climate model and the blocks of the experiments. Shaded area refers to the values between the (dotted) minimum and maximum values. Results shown are without an average moving window. Note that for FAST I, Block A was excluded from the analysis. The Austrian LTE, HOLL, consists of three Blocks only (A–C). **Figure S18:** Simulated surface runoff with SHP measured at Blocks A, B, C, and D in CENTS (DK), FAST I (CH) and HOLL (AT) per climate model and scenario. Full lines represent the median value between the repetitions within each climate model and shaded area refers to the values between the (dotted) minimum and maximum values. Results shown are without an average moving window. Note that for FAST I, Block A was excluded from the analysis. The Austrian LTE, HOLL, consists of three Blocks only (A–C). **Table S1:** Calibrated crop parameters for the conventional treatments, that is, (inversion) tillage and straw removal. Models were calibrated based on observed crop yield ($t\,ha^{-1}$).